ACTA RADIOLOGICA
EDITA IUSSU SOCIETATUM RADIOLOGICARUM
DANIAE, FENNIAE, NORVEGIAE ET SUECIAE

VOL. 51 JANUARY 1959 FASC. 1

LATERAL INTRATHORACIC MENINGOCELE

by

Roland Bunner

A lateral intrathoracic meningocele is a sacciform protrusion of the dura through an enlarged intervertebral foramen which then projects anteriorly between the ribs into the thoracic cavity and displaces the posterior part of the parietal pleura forwards. Its extension is, therefore, similar to that of hourglass tumours. These meningoceles are extremely rare and hence are apt to be overlooked in the differential diagnosis of intrathoracic tumours.

A study of the literature indicates that 20 cases have so far been reported. However, in three of them, *i. e.* the two communicated by CABELLO-CAMPOS and one of those described by HACKENSELLNER & PAPE, neither myelography, operation, nor autopsy served fully to verify the diagnosis; the roentgenologic findings nevertheless made it virtually certain.

The first case was reported by POHL in 1933. His patient was submitted to operation on the diagnosis of neurofibroma and a meningocele was found and excised; the patient died from empyema and meningitis a few days later, following the escape of cerebrospinal fluid into the pleural cavity.

Only in four cases (21, 9, 8, 2) has meningocele been diagnosed preoperatively, and in these varying methods were employed. SCHÜLLER &

Submitted for publication 30 May 1958.

From the Roentgen Department (Director: Docent Bengt Holmgren) Sabbatsbergs Sjukhus, Stockholm, Sweden.

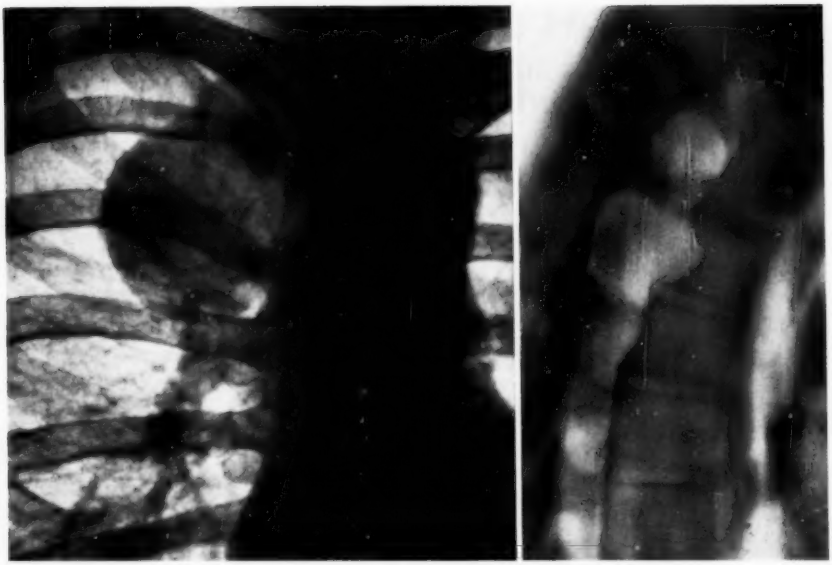

a b

Fig. 1. Case 1. a) Right polycyclic homogeneous growth. Enlargement of right fifth intercostal space. Erosions of the ribs and vertebrae at the level of the growth. Thoracic scoliosis. b) Lateral tomogram of thoracic spine. Enlargement of the intervertebral foramina and excavations posteriorly in the vertebral bodies at the same level. Slight kyphosis.

Uiberall were the first to diagnose a case of lateral intrathoracic meningocele preoperatively, which they did by means of suboccipital myelography, using Lipiodol as contrast medium. Cross, Raevis & Saunders carried out myelography with oil and air. Cmyral established the diagnosis in his case by puncturing the meningocele and injecting Lipiodol. Lastly, in one of the two cases communicated by Baker & Curtis myelographic examinations were made preoperatively with Pantopaque and Lipiodol.

All of the remaining 13 verified cases were diagnosed only at operation or autopsy. In most of the surgically treated cases the intrathoracic growths observed at preoperative roentgen examination had been regarded as neurofibromas with an intraspinal extension — hourglass tumours.

We have had two cases of lateral intrathoracic meningocele at our hospital. In both of them the diagnosis was made by means of pneumomyelography with suboccipital puncture of the subarachnoid space and injection of oxygen as contrast medium. In the first case an hourglass tumour with a large extraspinal part was suspected prior to myelography;

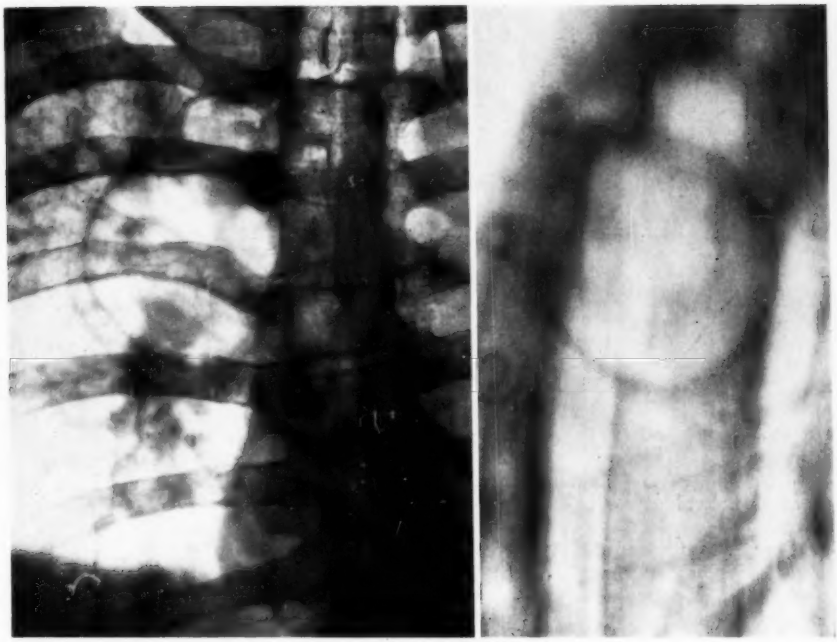

a b

Fig. 2. Case 1. Two contiguous meningoceles filled with oxygen at myelography. a) Frontal view. Medial flattening of the bases of the vertebral arches better visible than in fig. 1. b) Lateral tomogram.

in the other, the differential diagnosis lay between an hourglass tumour and a meningocele. We chose pneumomyelography with a view to establishing the extent of any intraspinal tumour that might have been present as well as to ascertain whether it involved or otherwise affected the spinal cord. In addition the gas, when it fills a meningocele, may afford useful information as to the latter's size, shape, and contents, and the thickness of its walls. Oxygen, moreover, is superior to oil for myelography, insofar as it is quite innocuous and rapidly absorbed, whereas oil is difficult to remove.

In view of the extremely rare occurrence of lateral intrathoracic meningoceles, details of these two cases are presented below.

Case 1. Woman, aged 43. A 'mass miniature' examination of the chest on 14 February 1952, showed a right-sided intrathoracic growth; prior to this she had never undergone roentgen examination. She felt well and had no cough. Recklinghausen's neurofibromatosis was present in the form of large and small areas of pigmentation, as well as hazel-

nut-sized skin tumours on the forehead and lateral surface of the left lower leg. Patellar and Achilles reflexes positive and Babinski's reflex doubtful bilaterally. Otherwise no neurologic symptoms or signs. Blood values, including sedimentation rate, normal.

Roentgen examination of lungs and thoracic vertebrae. A right paravertebral rounded and homogeneous soft tissue opacity, 6 to 7 cm in diameter, was present at the level of Th 5—6. Immediately cranial to this a similar opacity just over 2 cm in diameter was noted. The right fifth intercostal space was enlarged posteriorly and the posterior medial parts of the fourth, fifth and sixth ribs were eroded. There was moderate right scoliosis of the thoracic spine with its vertex at the level of Th 6 together with somewhat increased thoracic kyphosis. The intervertebral foramina between Th 4, 5 and 6 on the right side were enlarged and the vertebral bodies of Th 4, 5 and 6 — especially the fifth — were eroded. The bases of the arches at the level of the soft tissue tumours were flattened medially, *i. e.* the vertebral canal was enlarged.

The examination accordingly showed a growth of the soft parts, which was tentatively assumed to be an hourglass tumour. Pneumomyelography was then performed in order to elucidate the extent of its intraspinal portion. In this procedure a large volume of cerebrospinal fluid — 180 ml — was tapped and replaced by oxygen, which filled the paravertebral opacities. The latter thus consisted of meningoceles, protruding through two contiguous, enlarged intervertebral foramina. The spinal cord was observed to be quite intact at the level of the meningoceles and the areas of destruction.

Since the patient's condition was completely asymptomatic, no surgical measures were undertaken.

Case 2. Man, aged 36. At a 'mass miniature' examination in February 1956, an apical intrathoracic growth was detected on the right of the vertebral column. There had been no previous roentgen examination of the lungs. Apart from occasional slight cough during the previous six months he had been free from symptoms and his general condition was good. Clinical examination showed Recklinghausen's neurofibromatosis consisting of pea-sized skin fibromas, some of them pendulous, scattered over the whole body, as well as subcutaneous fibromas up to 5 mm wide. No neurologic symptoms or signs. Blood picture and sedimentation rate normal.

Roentgen examination of lungs and thoracic vertebrae. Rounded homogeneous soft tissue growth sharply defined in relation to the lung, with a right paravertebral localization at the level of Th 3, 4, and 5. The right third intercostal space was enlarged posteriorly and medially, with erosions in the upper medial part of the fourth rib and a small erosion in the lower medial part of the third rib. The right posterior aspects of the bodies of Th 3, 4, and 5 showed erosions in the form of excavations, most marked in Th 4. The right intervertebral foramina between Th 3 and 4, and Th 4 and 5 were enlarged. There was a slight right scoliosis of the upper portion of the thoracic spine. Diagnosis: neurinoma (hourglass tumour) or meningocele. At pneumomyelography about 180 ml of cerebrospinal fluid was tapped and replaced by oxygen; this filled the paravertebral mass, which accordingly consisted of a meningocele; its diameter was about 5 to 6 cm. The spinal cord was seen to be intact at the level of the meningocele.

The patient was asymptomatic throughout his stay in hospital and hence no operation was considered.

Discussion

Both of the above are typical cases of lateral intrathoracic meningoceles, most of which have a completely asymptomatic course. Each of them was detected incidentally at mass roentgen examination, and only

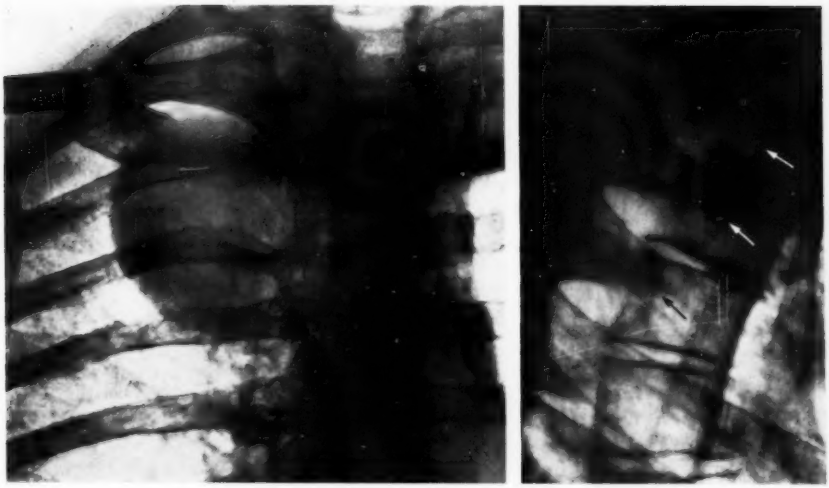

a b

Fig. 3. Case 2. a) Rounded homogeneous paravertebral growth on right side. Erosions in the right third and fourth ribs. The third intercostal space is enlarged. b) Appreciable excavations posteriorly in the bodies of the thoracic vertebrae at the level of the meningocele.

the second patient reported an occasional slight cough for about six months before the examination. Of the twenty cases previously reported, only a few were stated to have had symptoms. However, not all these symptoms could be definitely attributed to the meningoceles and the attendant destruction of bone; most of them consisted of pain in the head, thorax or lumbar region. Large meningoceles may produce symptoms of compression referable to intrathoracic organs, such as dyspnea, cough, and cardiac embarrassment.

The sex distribution seems to be approximately equal: of the aforementioned 20 cases, 9 were males and 9 females, the remaining 2 being infants whose sex was not stated. The age on detection of the meningocele was between 40 and 60 in ten cases, and over 60 years in three cases. The oldest patient was a 68-year-old woman; the youngest, apart from the two infants, an 11-year-old boy.

As regards the localization, the meningoceles were situated in the right thorax in 14 cases, including the present two. In 3 cases they were bilateral, though chiefly protruding to the right; in 2 the side was not reported, and in three cases the left thorax was involved.

The meningoceles varied in diameter from only a few centimeters to 'huge', the last-named description being given to one that occupied most

of one half of the thorax in an infant. Otherwise the diameters were mostly below 10 cm.

Recklinghausen's neurofibromatosis is a strikingly frequent concomitant, having been reported in 14 of the published cases, the present two included. Moreover, spinal deformities have been described in most cases of intrathoracic meningoceles: kyphosis and scoliosis, erosions of vertebral bodies and arches and of ribs, enlarged intervertebral foramina, and concavity of the dorsal surfaces of the vertebral bodies. Other reported anomalies include fused vertebrae, cuneate vertebrae, hemivertebrae with aplasia of the corresponding ribs and spines, and club foot.

It is chiefly the posterior excavations in the vertebrae at the level of the meningocele that have been noted by several earlier authors (1, 2, 8, 9, 11, 15). The skeletal lesions attending intrathoracic meningoceles are similar to those found in neurofibromatosis. Pathologic changes of the vertebral column in neurofibromatosis have been described by MILLER and by HAGELSTAM, among others. The first-named author found among 41 cases of Recklinghausen's neurofibromatosis varying degrees of osteoporosis in 23, and spinal involvement such as kyphosis, scoliosis and kyphoscoliosis in 16. In one case he described dorsal compression and erosions of vertebrae. In his opinion the kyphoscoliosis may be due to osteoporosis and muscular weakness, which is common in neurofibromatosis. HAGELSTAM collected from the literature 94 cases of Recklinghausen's neurofibromatosis with similar spinal changes. BRAUN has pointed out that the dorsal excavations may occur as an independent sign without intrathoracic meningocele in Recklinghausen's neurofibromatosis. The skeletal changes demonstrate the association between intrathoracic meningoceles and Recklinghausen's disease.

If a paravertebral intrathoracic tumour is found concomitantly with neurofibromatosis, it would be logical to regard the neoplasm tentatively as a neurofibroma. Yet, neurofibromatosis is in fact uncommon in intrathoracic neurogenic tumours: KENT, BLADES, VALLE & GRAHAM found only four cases among 105 with such tumours; BLADES had one case out of 30 with neurogenic tumours; HAGELSTAM had two neurinomas among his 94 cases of neurofibromatosis associated with spinal changes. Hence neurofibromatosis coexists with intrathoracic meningocele more commonly than with neurinoma.

Intrathoracic meningocele should thus be suspected whenever a paravertebral intrathoracic tumour is associated with Recklinghausen's neurofibromatosis and spinal abnormalities such as kyphoscoliosis, enlarged intervertebral foramina, and erosions of the vertebrae, notably excavations posteriorly. The method of examination that gives an assured diagnosis and the best information is pneumomyelography. Indeed, with

Fig. 4. Case 2. Tomogram through the central part of the oxygen-filled meningocele at myelography.

this procedure the diagnosis of meningocele may already be made, or at all events strongly suspected, on tapping the cerebrospinal fluid, due to the large volume withdrawn. In each of the two present cases, this volume amounted to about 180 ml.

The etiology of intrathoracic meningocele is unknown, though many theories have been advanced. CMYRAL referred to primary weakness of the dura, which may lead secondarily to meningocele. SENGPIEL, RUZICKA & LODMELL and MENDELSON & KAY believed that anomalies of the dural attachment in the intervertebral foramina may be the cause and, together with variations in the cerebrospinal fluid pressure, may give rise to meningocele. Fluid pulsations may even cause the posterior excavations in the vertebral bodies, according to HACKENSELLNER & PAPE and BYRON et coll., who found in their cases that the dura was contiguous with the posterior surfaces of those bodies. Normally the dura and the bone are separated by loose connective tissue that absorbs the waves of pressure in the cerebrospinal fluid. In the absence of this connective tissue, the posterior excavations might conceivably arise. The epiphysial disks have greater powers of resistance and are not affected. A decreased resistance in the bone structure (MICHAELIS) and trophoneurotic disturbances of skeletal growth (HAGELSTAM) are conducive to bone lesions and secondary meningoceles.

In some cases, growth of the intrathoracic meningocele has been reported. In the case communicated by AMEUILLE, WOLMOTH & KUDELSKI the meningocele had increased in size, concurrently with progression of the skeletal lesions, over a follow-up period of 11 years, and at the time of operation it had a diameter of 8 cm. In CIAGLIA's case, chest roentgenograms had been taken two years before detection of the meningocele but had shown nothing pathologic. Lastly, BYRON et coll. reported in one of their cases progression of the meningocele, over a 6-year period, from a sac 10 cm in diameter to such a volume as to fill two-thirds of one half of the thoracic cavity.

Of the seven patients who underwent surgical removal of the meningocele, one died of pleural empyema and meningitis due to escape of cerebrospinal fluid into the pleura (POHL). In the other six cases the postoperative course was on the whole uneventful. In none of these cases was any recurrence reported, although the longest observation time amounted to only 3 1/2 years (CIAGLIA).

In one case (AMEUILLE et coll.) the meningocele was treated by puncture, then covered with parietal pleura; but here too cerebrospinal fluid escaped into the pleura and the patient died a week or so later from pleural empyema and meningitis. In yet another patient it was sought to remove the meningocele operatively (BYRON et coll.), but death occurred from cardiac failure during the operation.

Each of the six successful operations has been performed since 1948; *i. e.*, various antibiotics have been available and the operative technique has advanced.

Opinions diverge as to the advisability of surgical treatment for intrathoracic meningoceles. MENDELSON & KAY caution against operation unless the meningocele progresses and gives rise to symptoms. They write: 'The defect is difficult to repair satisfactorily and might be associated with a high incidence of recurrence.' BYRON et coll. hold the same view. According to BAKER & CURTIS the indications for operation are: continued enlargement of the meningocele, compression of intrathoracic organs, and progressive erosion of contiguous vertebrae.

SUMMARY

Two cases of intrathoracic meningocele, diagnosed by pneumomyelography, are reported. The cases were typical in being without symptoms and being associated with Recklinghausen's neurofibromatosis and spinal lesions. The question of surgical treatment is discussed.

ZUSAMMENFASSUNG

Zwei Fälle mit intrathorakaler Meningocele, welche pneumomyelographisch diagnostiziert worden sind, werden berichtet. Die Fälle waren typisch. Sie hatten keine Symptome und waren mit der Recklinghausenschen Neurofibromatose und spinalen Veränderungen verbunden. Die chirurgische Behandlung wird diskutiert.

RÉSUMÉ

L'auteur présente deux cas de méningocèle intrathoracique diagnostiqués par myélographie gazeuse. Ces cas étaient typiques par leur absence de symptômes et par leur association à une neurofibromatose de Recklinghausen et à des lésions rachidiennes. L'auteur examine la question du traitement chirurgical.

REFERENCES

1. Ameuille, P., Wilmoth, P. et Kudelski, Ch.: Meningocèle rachidienne à développement intrapleural. Bull. Soc. méd. Hôp. Paris 56 (1940), 608.
2. Baker, J. M. and Curtis, G. M.: Intrathoracic meningocele. West. J. Surg. 61 (1953), 209.
3. Blades, B.: Mediastinal tumors. Amer. J. Surg. 123 (1946), 749.
4. Braun, H.: Die dorsale Wirbelexkavation, ein selbständiges Symtom bei der Neurofibromatose Recklinghausen. Fortschr. Röntgenstr. 83 (1955), 844.
5. Byron, F. X., Alling, E. F. and Samson P. C.: Intrathoracic meningocele. J. thorac. Surg. 18 (1949), 294.
6. Cabello-Campos, J. M.: Meningocele intrathoracico. Bol. San. Lucas 8 (1946), 40.
7. Ciaglia, P.: Intrathoracic meningocele. J. thorac. Surg. 23 (1942), 283.
8. Cmyral, Rudolf: Über einem Fall von intrathoracaler bilateraler Meningocele. Radiol. Austriaca 5 (1952), 23.
9. Cross, G. O., Raevis, J. R. and Saunders, W. W.: Lateral intrathoracic meningocele. J. Neurosurg. 6 (1949), 423.
10. Goldman, J. Ralph: Congenital malformation of vertebrae (hemivertebrae) with aplasia of corresponding ribs, associated with a lateral meningocele. Arch. Pat. 7 (1949), 153.
11. Hackensellner, H. A. und Pape, R.: Über Meningkelen bei Neurofibromatosis Recklinghausen. Fortschr. Röntgenstr. 81 (1954), 65.
12. Hagelstam, Lars: On deformities of spine in multiple neurofibromatosis. Acta chir. scand. 93 (1946), 169.
13. Kent, E. M., Blades, B., Valle, A. R. and Graham, E. A.: Intrathoracic neurogenic tumors. J. thorac. Surg. 13 (1944), 116.
14. Lindgren, Erik: *In:* Röntgenologie. Handbuch der Neurochirurgie. Hrsgeg. von H. Olivecrona und W. Tönnis. Band II. Springer, Berlin 1954.
15. Mendelson, H. I. and Kay, E. B.: Intrathoracic meningocele. J. thorac. Surg. 18 (1949), 124.
16. Michaelis, L.: Über Wirbelsäulenveränderungen bei Neurofibromatose. Beitr. Bruns' klin. Chir. 150 (1930), 574.
17. Miller, G.: Knochenveränderungen bei Neurofibromatosis. Fortschr. Röntgenstr. 78 (1953), 1.
18. Ottani, G.: Intrathoracic meningocele. Ann. Radiol. diagn. (Bologna) 23 (1951), 416.
19. Pohl, R.: Meningocele im Brustraum. Röntgenpraxis 5 (1953), 707.
20. Rubin, S. and Stralemeyer, E. H.: Intrathoracic meningocele. Radiology 58 (1952), 552.
21. Schüller, A. and Uiberall, H.: A case of neurofibromatosis Recklinghausen combined with lateral spinal meningocele. Confin neurol. 1 (1938), 312.
22. Sengpiel, G. W., Ruzicka, F. F. and Lodmell, E. A.: Lateral intrathoracic meningocele. Radiology 50 (1948), 515.
23. Welch, C. S., Ettinger, A. and Hecht, P. L.: Recklinghausen's neurofibromatosis associated with intrathoracic meningocele. New Engl. J. Med. 238 (1948), 622.

FROM THE ROENTGEN DEPARTMENT (DIRECTOR: PROF. ERIK LINDGREN), SERAFIMERLASARETTET, STOCKHOLM, SWEDEN

CIRCULATION THROUGH THE POSTERIOR COMMUNICATING ARTERY IN DIFFERENT COMPRESSION TESTS

A preliminary report

by

Georg-Fredrik Saltzman

According to the literature the posterior cerebral artery is filled in one third to one fifth of all carotid angiographies. Anatomical investigations have shown, however, that the posterior communicating artery is seldom absent on any side, but in spite of this it would appear that no contrast medium passes through the posterior communicating artery in the majority of carotid angiographies.

The situation is the same regarding the anterior communicating artery. It is, however, well known to all neuroradiologists that it is possible in nearly all cases to direct blood through the anterior communicating artery to the other half of the brain by compression of the contralateral carotid artery at the time of the injection. This method has achieved great practical importance, particularly in cases in which prior to operation the risk of being forced to interrupt the normal supply of blood has to be considered. No similar method of directing or increasing the flow of blood from the carotid artery through the posterior com-

Submitted for publication 10 June 1958.

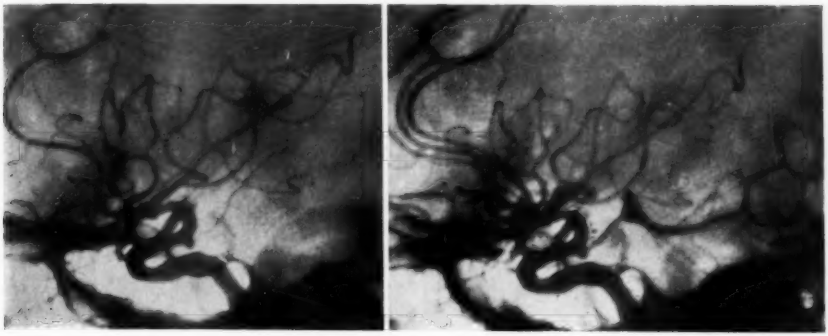

a b

Fig. 1. Unilateral compression of the vertebral artery in carotid angiography. a) Before the compression the posterior cerebral artery is not filled. b) After compression the artery is well filled.

municating artery to the posterior cerebral artery has so far been described.

ENGESET writes: 'Theoretically it would seem that bilateral compression of the vertebral artery would force the blood-stream from the carotid syphons to the basilar trunk.' That this is indeed the case is demonstrated in practice by the fact that patients have survived bilateral ligature of the vertebral artery. No report of a practical routine method of compression of the vertebral artery has, however, appeared.

The vertebral artery from its origin in the subclavicular artery at first runs in front of the spine and from the sixth cervical vertebra normally passes through the transverse foramina. Topographic studies on cadavers indicate that in most cases at least it would be possible to affect the vertebral artery by manual compression immediately above the clavicle.

In the compression experiments described below the following technique has been employed. One finger is introduced immediately above the clavicle behind the common carotid artery and directed inwards; when the finger has covered about two centimeters of a transverse process, it is firmly pressed, still in the same position, against the process.

The first experiments were made with unilateral compression of the vertebral artery. The circulation through the basilar artery obviously cannot be arrested by unilateral compression, but one would expect a certain lowering of the pressure in this vessel and its branches. In 18 experiments, good contrast-filling of a posterior cerebral artery, which had not filled without compression, was obtained in one case (Fig. 1). In 2 other cases slight filling of the posterior cerebral artery was obtained

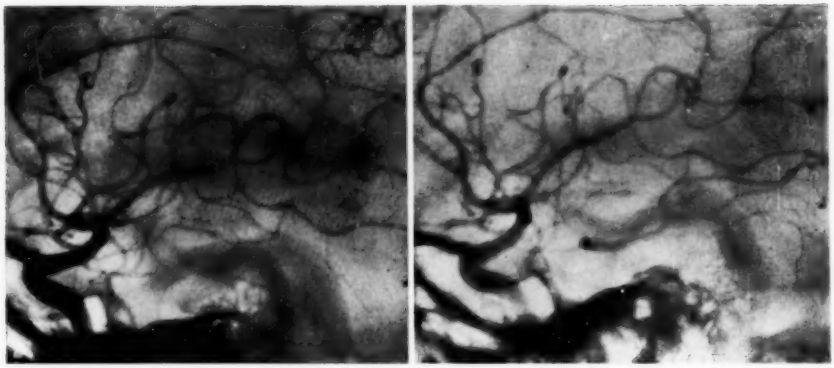

a b

Fig. 2. Bilateral compression of the vertebral artery in carotid angiography. a) Before compression, no filling of the posterior cerebral artery. b) Dense contrast-filling after the compression.

without compression, and considerably denser filling after compression; in the remaining cases no definite difference could be observed.

Bilateral compression of the vertebral artery was attempted in 10 cases. Four of these experiments were successful: in 2 of them no contrast-filling of the posterior cerebral artery was obtained before compression, but dense filling following it (Fig. 2). In a third case, in which the posterior cerebral artery did not fill without compression, filling was obtained after compression not only of this vessel but also to some extent of the basilar artery. In the fourth case, thin and fragmentary contrast-filling of the posterior cerebral artery was observed before compression. After compression the artery was densely filled with contrast medium, and, furthermore, the medium filled the basilar artery in a retrograde direction. Some cerebellar branches were also outlined (Fig. 3).

Compression of the vertebral artery was undertaken in all cases in connection with standard examinations and, in order not to administer contrast medium in unnecessarily large amounts only one compression experiment was performed in each.

The greatest difficulty in compression of the vertebral artery appears to lie in avoiding compression of the carotid artery at the same time so that the desired difference in pressure is not lost. Considerable difficulties of this nature have been encountered in patients with very narrow necks. It is also important not to change the position of the injection needle in the carotid artery during the compression. WICKBOM and RUGGIERO have pointed out how difficult it is to obtain filling of the anterior cerebral artery when the position of the needle is not correct. An unsatisfactory

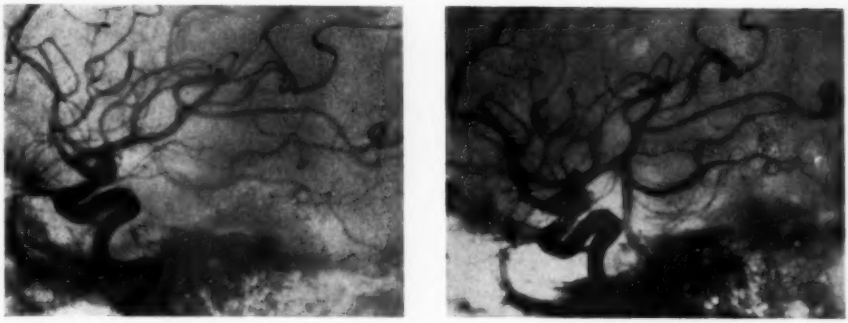

a b

Fig. 3. Bilateral compression of the vertebral artery in carotid angiography. a) Before compression, fragmentary filling of the posterior cerebral artery. b) After compression, dense contrast-filling of the posterior cerebral artery, and filling also of the basilar artery and some cerebellar branches.

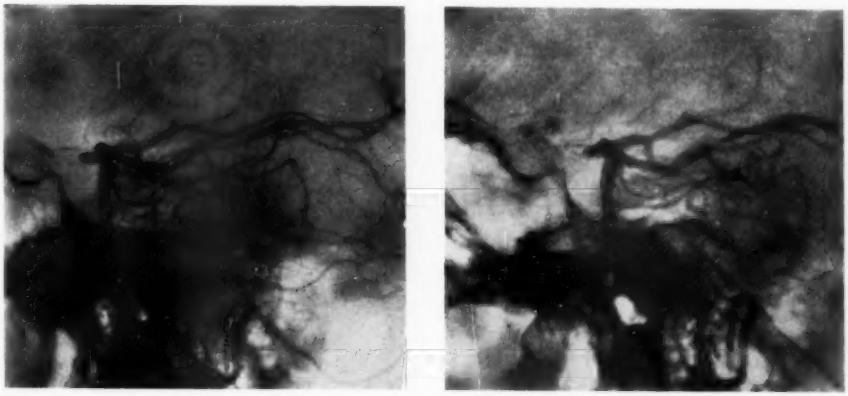

a b

Fig. 4. Compression of the carotid artery in vertebral angiography. a) Before compression, no contrast medium in the carotid syphon. b) After compression contrast medium is visible in the syphon.

needle position appears to have the same effect on the passage of contrast medium through the posterior communicating artery.

Successful compression of the vertebral artery may well become a useful diagnostic aid and should facilitate the diagnosis of expanding processes within the area of the posterior cerebral artery. Tentorial herniations may be mentioned as one example and AZAMBUJA, LINDGREN and SJÖGREN have described a characteristic displacement of the posterior

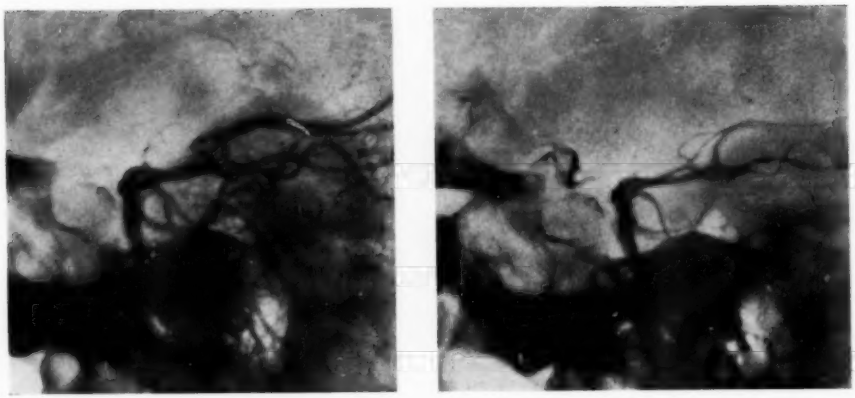

a b

Fig. 5. Compression of the carotid artery in vertebral angiography on opposite side to the puncture. a) Before compression no contrast medium in the carotid syphon. b) After the compression, contrast medium is present.

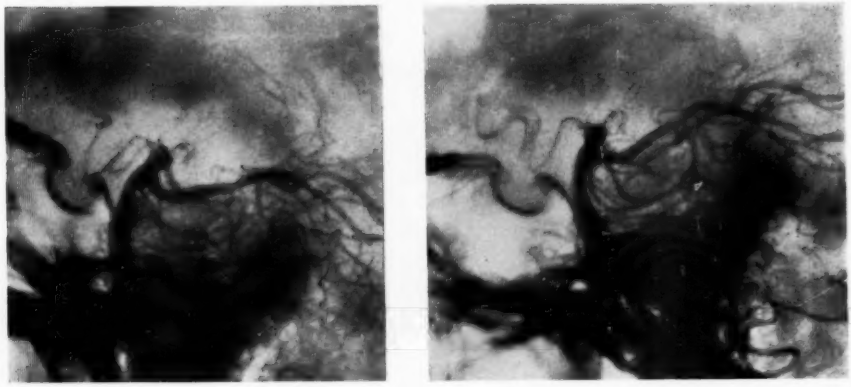

a b

Fig. 6. Compression of the carotid artery in vertebral angiography on opposite side to the puncture. More contrast medium visible in the carotid syphon after the compression (b) than before (a).

cerebral artery in such herniations. If compression of the vertebral artery produces a substantial increase in the number of cases in which the posterior cerebral artery is filled this sign will achieve added importance. Another field in which compression of the vertebral artery may become of value is the mapping-out of the vascular supply of supratentorial

arteriovenous malformations. One of our cases (Fig. 3) suggests the possibility of examining vessels of the vertebral area other than the posterior cerebral artery by means of carotid angiography. It is too early to state whether this can be done to any greater extent.

The verification of a free passage through the anterior communicating artery has, as mentioned previously, become of great importance in neurosurgery but so far there has been no definite need for a corresponding examination of the posterior communicating artery. Should such a need arise compression of the vertebral artery may be employed.

The blood flow through the posterior communicating artery may, however, also be directed in the opposite direction, as shown by KRAYENBÜHL and YAŞARGIL. Technically successful vertebral angiographies have been combined with compression of the carotid artery in 4 cases, in all of which contrast medium passed from the posterior cerebral artery through the posterior communicating artery to the carotid syphon; in 2 of these the carotid artery was compressed on the same side as the vertebral puncture (Fig. 4), and in the other two cases on the opposite side (Figs. 5 and 6).

The position of the needle in vertebral angiography is always more or less unstable. Compression of the carotid artery should therefore be performed with the greatest caution, so that the contrast medium is not injected paravasally or into the wall of the vessel; compression of the carotid artery on the opposite side is to be preferred. The risks will naturally be considerably diminished when a catheter is employed for the vertebral angiography.

SUMMARY

A method of compressing the vertebral artery between its origin in the subclavicular artery and the point where it enters the transverse foramen of the sixth cervical vertebra is described. By this means filling of the posterior cerebral artery in carotid angiography is rendered possible. The diagnostic importance is discussed. Compression of the carotid artery in vertebral angiography, by which the passage of contrast medium through the posterior communicating artery may be studied, is also described.

ZUSAMMENFASSUNG

Eine Methode, die Arteria vertebralis zwischen ihrem Beginn in der Arteria subclavia und der Stelle, an der sie in das Foramen transversum des 6. Halswirbels eintritt, zu komprimieren, wird beschrieben. Auf diese Weise wird die Füllung der Arteria cerebralis posterior bei der Karotisangiographie möglich gemacht. Die diagnostische Bedeutung wird besprochen. Die Kompression der Arteria carotis bei der Vertebralisangiographie, durch welche der Durchgang des Kontrastmittels durch die Arteria communicans posterior studiert werden kann, wird ebenfalls beschrieben.

RÉSUMÉ

L'auteur décrit une méthode de compression de l'artère vertébrale entre son origine dans l'artère sous-clavière et le point ou elle pénètre dans le trou transversaire de la sixième vertèbre cervicale. Cette méthode permet de rendre visible l'artère cérébrale postérieure par angiographie carotidienne. L'auteur en examine l'intêret diagnostique. Il décrit aussi la compression de l'artère carotide au cours de l'angiographie vertébrale, qui permet d'étudier le passage du moyen de contraste à travers l'artère communicante postérieure.

REFERENCES

Azambuja, N., Lindgren, E. and Sjögren, S. E.: Tentorial herniations. III. Angiography. Acta radiol. 46 (1956), 232.

Engeset, A.: About the angiographic visualization of the posterior cerebral artery, especially by intracarotid injection of contrast. Acta radiol. 30 (1948), 152.

Krayenbühl, H. and Yaşargil, M. G.: Die vasculären Erkrankungen im Gebiet des Arteria vertebralis und Arteria basilaris. Georg Thieme Verlag, Stuttgart 1957.

Ruggiero, G.: Factors influencing the filling of the anterior cerebral artery in arteriography. Acta radiol. 37 (1952), 87.

Wickbom, I.: Angiography of the carotid artery. Acta radiol. (1948) Suppl. 72.

FROM ROENTGENDIAGNOSTIC DEPARTMENT B (DIRECTOR: DOCENT N. P. G. EDLING),
KAROLINSKA SJUKHUSET, STOCKHOLM, SWEDEN

NEPHROGRAPHIC EFFECT IN RENAL ANGIOGRAPHY

An experimental study in dogs

by

N. P. G. Edling and *C. G. Helander*

The nephrographic effect in urography and in renal angiography is in both instances caused by an accumulation of the contrast medium within the renal tissues. The mechanism of this phenomenon occurring during urography has been studied by EDLING et coll. (1954, 1957) who found it to depend upon the reduction of the glomerular filtration pressure, and stasis within the tubules, due either to a fall in blood pressure caused by shock or to back pressure within the renal pelvis resulting from ureteral stasis. The plasma concentration of the contrast medium within the renal vessels is low and plays no significant part in the increased density of the organ; the glomerular filtration has more or less ceased and the tubular function alone plays the main role in the nephrographic effect in urography.

At renal angiography EDSMAN (1957) attributes an equal role in the nephrographic effect to the contrast medium which fills the vessels and also accumulates in the excretory system; in the beginning, the accumulation of the contrast medium is mostly confined to the capillaries of the cortex, later moving to the nephrons and adjacent cells. VOGLER & HERBST (1958) describe the nephrographic effect in angiography as merely the summation of the contrast-filling in the capillaries.

Submitted for publication 3 May 1958.

In order to study the different components causing the increase in density of the renal tissue in angiography the writers have studied the nephrographic effect experimentally in 19 healthy dogs (between 15.2 and 27.5 kg).

The dogs were kept under light general anesthaesia. The contrast medium injections were performed following transfemoral catheterization either into the aorta or into a renal artery (EDHOLM & SELDINGER 1956). The media used were di- or triiodine compounds (Umbradil, Miokon, or Urografin) except in one examination. At the aortographies, 40 to 100 ml Miokon 50 % or Urografin 60 % were injected at a speed of approximately 8 to 10 ml/second, and at the selective angiographies 3 to 8 ml Umbradil 35 %, or 50 %, or Miokon 30 %, at a speed of about 5 ml/second. At one bilateral selective renal catheterization 8 ml Miokon 50 % and 8 ml Thorotrast were injected simultaneously into the right and left renal arteries, respectively. The injection time in this animal was about 6.5 seconds, amounting to 1.2 ml/second. This examination was repeated.

Exposures were made by means of an automatic film changer (GIDLUND 1956), a manual 4-film changer, or on single films. When the automatic film changer was used the exposures were 2 per second for 8 seconds, 1 per second for 8 seconds, and 1 every 3 seconds.

Aortography was performed in 8 dogs in whom both kidneys were studied, bilateral selective renal angiography in 6 dogs, and unilateral selective angiography in 5 dogs — making a total of 33 kidneys examined.

Results

In 6 dogs (11 kidneys) examined by means of the automatic film changer the time intervals could be determined and the components of the nephrographic effect studied in relation to time.

Legend to illustration on opposite page.

Selective injections of 8 ml Miokon 50 % into the right renal artery, and 8 ml Thorotrast into the left renal artery in a dog. The exposures were made, from commencement of injections, at the times indicated on the separate views. The injections were completed after 6 1/2 seconds.

1 sec: The renal arteries and their branches are visible. Density of kidneys slightly increased.

1 1/2 sec: Increasing density of the kidneys, in the right one especially in the cortex.

3 1/2 sec: Further increasing density, mostly in the right kidney. Commencing contrast-filling of the left renal vein.

7 sec (immediately following end of injections): Arteries no longer visible. Density of right kidney still further increased. Filling of renal vein commencing. Density of left kidney decreasing. The renal vein and its branches are filled with contrast medium of high concentration.

10 sec: Right kidney is now very dense. Low density of renal vein. Density of left kidney further decreased. Renal vein still very poorly filled.

27 sec: Density of right kidney has now decreased, especially in the cortex. The renal vein is faintly visible. Excretion of Miokon in left kidney.

45 sec: In the right kidney the density of cortex is very low compared with the pyramids which are still clearly visible. Left kidney unchanged.

69 sec: Both kidneys have now about the same density as the surrounding soft tissue. Excretion of Miokon in both.

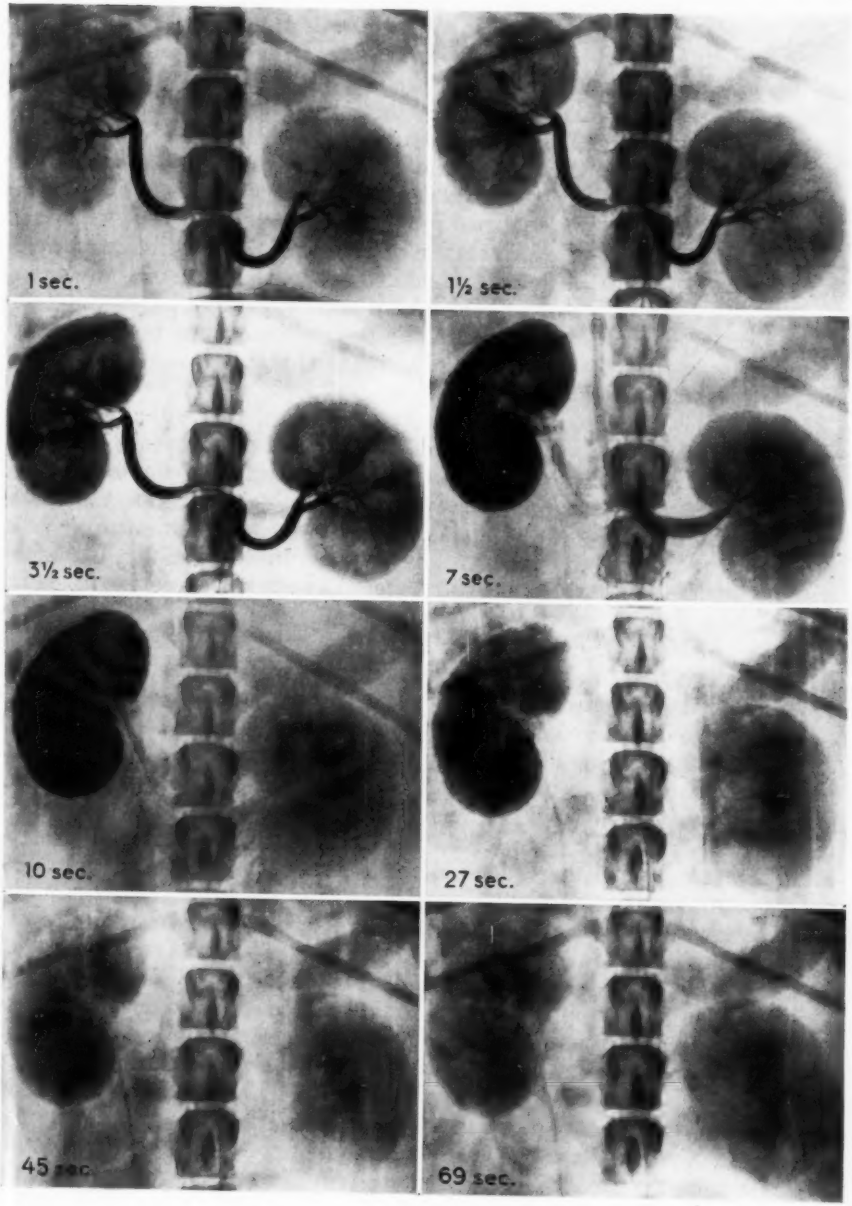
1 sec.
1½ sec.
3½ sec.
7 sec.
10 sec.
27 sec.
45 sec.
69 sec.

The dog injected simultaneously with both Miokon and Thorotrast is of special interest and will be described first. The doses of the contrast media injected had the same absorption capacity for roentgen rays. However, there is the important difference that Thorotrast is not excreted by the kidneys, either by the glomeruli or the tubules.

It was seen within the first second, in respect to both kidneys, that the renal arteries were of the same width and density, and a clear representation was obtained of the groups of interlobar arteries between the pyramids, and of a few interlobar arteries in the cortex (see the accompanying illustration on p. 19). The archiform arteries at the level of the bases of the pyramids were only just visible. After one second an increased density commencing in the cortex became visible on both sides; but from that moment onwards, however, the kidneys reacted in their own different ways.

The kidney injected with Thorotrast increased only moderately in density and the small vessels were clearly delineated. The renal vein was shown with considerable density after 3.5 sec. After the injection had been completed (6.5 sec) the density of the kidney decreased (without increased density of the pyramids). After 10 sec the renal tissue was of normal density and the renal veins were no longer visible. The small amount of Miokon in the renal pelvis was the result of excretion following a small test dose for catheter localization.

In the kidney injected with Miokon there was also an increase in density which within a few seconds reached a very high degree, especially in the cortex. The small vessels appeared less clearly than those in the left kidney. When the injection was completed (6.5 sec) the density was still increasing. The renal vein was just visible after 7 sec, at which time the pyramids began to increase in density, and after 10 to 17 sec there was a diffuse nephrographic effect of a very high degree. At about 27 sec the density of the cortex decreased, the pyramids became well defined, and the contrast medium in the renal vein was insufficient for adequate delineation; the cortex emptied, and at 45 sec the pyramid apices were well shown; these also gradually faded, and after 69 sec the kidney was of normal density. Only the excretion into the pelvis was visible.

All the contrast medium had thus disappeared in the left kidney in 10 seconds. The renal vein was visible for 6.5 seconds, *i. e.* as long as the duration of the injection. In the right kidney there was at first an accumulation of contrast medium followed by filling of the veins. The time interval between the commencement of the injection and the time when the density of the kidney was normal again was 69 seconds. The venous filling started later, was poor, and lasted 20 seconds, *i. e.* about 13 seconds longer than the injection time.

In the remaining five dogs (9 kidneys), also examined by means of the

automatic film changer, the progress of the nephrographic effect was the same in each case, the differences in degree and time depending upon the different quantities of contrast media injected and the injection rate. In one aortography, the contrast-filling of the renal veins was first discernible after 4 seconds and was visible for 30 seconds; the nephrographic effect, as described above, was still present after about 40 seconds, during which time good excretion was taking place. In seven selective renal angiographies, the renal veins became visible after 2 to 3 seconds and remained so for 6 seconds; the nephrographic effect was of moderate or low degree and lasted in no case more than 20 seconds. In all cases the contrast-filling of the arteries disappeared when the injection was completed.

In the remaining cases, exposed with one to four single films in each, the findings were approximately the same.

Discussion

The time interval between the commencement of the injection of Thorotrast into the renal artery and the appearance of contrast medium in the renal vein corresponded to the time interval between the end of the arterial injection and the disappearance of visible contrast medium from the renal vein. These equal intervals correspond to the circulation time in the kidney under the experimental conditions. The increase of the density of the renal tissue lasted only as long as the concentration of medium in the capillaries was capable of producing a density of higher degree than that of the soft tissue alone. This is not characteristic of renal tissue and the findings indicate that the initial contrast-filling of the vessels alone is of only temporary importance for the density in the nephrographic effect in angiography.

In the other kidney of the same animal, injected with the organic iodine compound, the renal vein was demonstrated in the first instance later, *i. e.* at the end of the injection and it was less dense and visible several seconds; in addition, the increase in the density of the renal tissue was much more intense and protracted. The delay and the low concentration of contrast medium in the vein depend upon its immediate accumulation in the kidney, both through the glomerular filtration and the tubular excretion into the tubules, and, when the kidney is supplied with such large quantities of contrast medium, the cells of the tubules are able also to store some of it (Engström & Josephson 1953). This explains why the amount of contrast medium remaining in the blood after the passage through the kidney is insufficient for a demonstration of the vein. This accumulation also explains why in renal angiographies with relatively small doses of contrast medium in man the renal vein is often not visible. In the present experiment, when the renal vein was visible for a long time

after the arterial injection had ceased, it was due to the extraction of the medium from the renal tissue. It seems that there can be only two possible sources: either the medium which was stored in the tubular cells or that which was filtered and excreted into the tubular ducts. After the supply of contrast medium had ceased, the blood entering the kidney had the same low contrast medium content as the blood elsewhere in the body. There was therefore, a marked difference in the concentration of contrast medium between the circulating blood and the tubular cells. It seems reasonable to suppose that back diffusion of the stored contrast medium takes place from the tubular cells into the blood, explaining the delayed filling of the renal vein. The second possibility is that there is a reabsorption of contrast medium into the blood occurring with water absorption from the tubules. This explanation, however, may probably be excluded since it is known from clearance studies that substances such as Diodrast and PAH are not reabsorbed from the tubules in healthy kidneys (SMITH 1951).

Even though it is not definitely known how the contrast medium returns to the blood after the injection has ceased to outline the vein, the conclusion may be drawn that back diffusion must have taken place. This is supported by investigations by JOSEPHSON et coll. 1952 who had indirect proof of a reabsorption back to the blood of substances stored in the tubular cells and designed for excretion.

The loss of the demarcation between cortex and medulla occurred when the contrast medium passed through the descending and ascending limbs of the pars recta of the tubules, the nephrographic effect being temporarily fairly homogenous. The density in the cortex then faded due to a decrease in the concentration of the contrast medium in the proximal tubules, following elimination of fluid of high concentration and the addition of a glomerular filtrate of much lower concentration. In addition, the tubular cells lose contrast medium from back diffusion into the blood and from excretion into the tubular ducts. Hence, the pyramids and finally the papilla have the highest density, indicating that the contrast medium has reached the collecting ducts. The nephrographic effect is finally lost with the emptying of the tubular ducts into the pelvis.

Essentially the same appearances and the same low concentration of contrast medium in the renal vein was found in the other timed experiments; there was however no delay in the filling of the renal vein. The difference is explained by the slowness of the injection of contrast medium in the dog that was injected with both Miokon and Thorotrast. When small test doses were injected the vein was not outlined at all.

Conclusions

This investigation demonstrates that for the true nephrographic effect to occur, the contrast medium must be excreted through the kidneys. The investigation also indicates that the nephrographic effect in renal angiography starts with an increase in the density of the kidney due to contrast-filling of the arteries, but in the main is dependent upon the filtration and excretion of the medium. However, since there is also back diffusion of the contrast medium from the tubular cells into the blood the venous contrast-filling plays a role in the increase in density. The last stage of the nephrographic effect results mainly from the contents of the tubular ducts. In brief, the nephrographic effect in angiography is made up of three stages: an initial vascular phase, a phase of tubular accumulation and excretion, and a phase of back diffusion into the veins and tubular transport. It therefore seems suitable to use the term 'angionephrographic effect' to indicate the nephrographic phenomenon in angiography.

SUMMARY

The nephrographic effect in renal angiography has been studied experimentally in dogs. The results indicate that the phenomenon in the main depends upon the contrast medium which is accumulated in the tubular cells and ducts, but to some degree also upon the contrast medium appearing in the veins after back diffusion from the tubular cells.

ZUSAMMENFASSUNG

Der nephrographische Effekt bei der renalen Angiographie ist bei Hunden experimentell untersucht worden. Die Ergebnisse zeigen, dass das Phänomen wesentlich auf dem in den Zellen der Nierenkanälchen und in den Nierengängen gespeicherten Kontrastmittel beruht; in gewissem Grade ist es jedoch auch abhängig vom Kontrast in den Venen, in welche dieser nach Rückdiffusion aus den Zellen der Tubuli gelangt.

RÉSUMÉ

Les auteurs ont étudié expérimentalement sur des chiens l'effet néphrographique dans l'angiographie rénale. Les résultats de leur travail montrent que ce phénomène est dû surtout au moyen de contraste accumulé dans les cellules des tubes et dans les canaux excréteurs; mais il est dû aussi, dans une certaine mesure, au moyen de contraste parvenu dans les veines après diffusion rétrograde à partir des cellules des tubes rénaux.

REFERENCES

EDHOLM, P. and SELDINGER, S. I.: Percutaneous catheterization of the renal artery. Acta radiol. 45 (1956), 15.

EDLING, N. P. G., HELANDER, C. G. and RENCK, L.: The correlation between contrast excretion and arterial and intrapelvic pressures in urography. Acta radiol. 42 (1954), 442.

— — and SELDINGER, S. I.: The nephrographic effect in depressed tubular excretion of Umbradil. Acta radiol. 48 (1957), 1.

EDSMAN, G.: Angionephrography and suprarenal angiography. Acta radiol. (1957) Suppl. 155.

ENGSTRÖM, A. and JOSEPHSON, B.: Historadiographic demonstration of Diodrast in the rabbit kidney. Amer. J. Physiol. 174 (1953), 61.

GIDLUND, Å.: Development of apparatus and methods for roentgen studies of haemodynamics. Acta radiol. (1956) Suppl. 130.

JOSEPHSON, B., BUCHT, H., EK, J. and WERKÖ, L.: Renal extraction, its depression and the tubular storage of PAH in the healthy and in the diseased human kidney. Scand. J. Clin. lab. Invest. 4 (1952), 1.

SMITH, H. W.: The kidney. Oxford University Press, New York 1951.

VOGLER, E. und HERBST, R.: Angiographie der Nieren. Georg Thieme Verlag, Stuttgart 1958.

FROM THE ROENTGENDIAGNOSTIC DEPARTMENT (DIRECTOR: PROF. K. LINDBLOM),
KAROLINSKA SJUKHUSET, STOCKHOLM, SWEDEN

PERCUTANEOUS SELECTIVE ANGIOGRAPHY OF THE SUPERIOR MESENTERIC ARTERY

by

Per Ödman

Selective angiography of the superior mesenteric artery with antegrade catheterization has already been described in the literature (BIERMAN et coll.). No special directions regarding technique have been given; nor does the method seem to have been used for diagnostic purposes, although some investigators have stressed the need for a more exact angiographic procedure in the diagnosis of mesenteric embolism (ODÉN & WALLENSTEN).

When the technique for selective percutaneous angiography of the coeliac artery was worked out, it was found that the superior mesenteric artery could be catheterized with the KIFA radiopaque polythene catheter, 'large' size, which has been modelled for the coeliac artery (ÖDMAN). This possibility has subsequently been utilized in angiographic studies. Catheterization is carried out in approximately the same way for both the superior mesenteric and coeliac artery. After percutaneous transfemoral insertion, and under fluoroscopic control, the catheter, which has a sharp bend at its distal end, is pushed into the abdominal aorta till it is considered to be lying immediately caudal to the pertinent vessel opening. The tip is then directed cranially along the ventral aortic wall till it is caught up in the mouth of the artery. The procedure is controlled by fluoroscopy from the side.

Submitted for publication 9 June 1958.

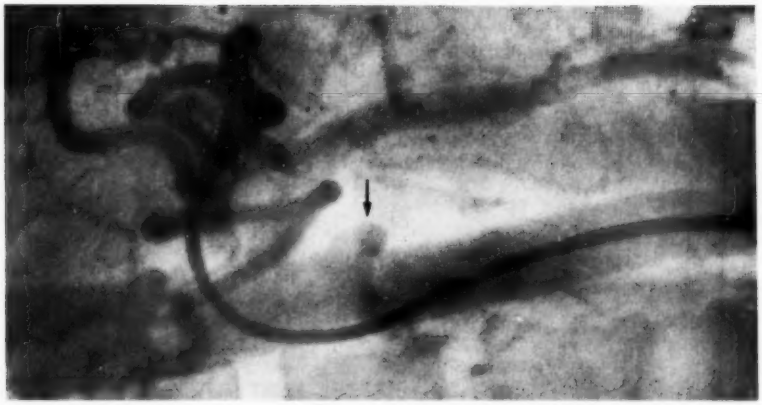

Fig. 1. Lateral view. Abdominal aorta narrows at origins of visceral branches. Central parts of renal arteries (→) lie ventral to aorta.

The following features should be borne in mind in connection with the examination of the superior mesenteric artery. The abdominal aorta narrows considerably at the origin of the large visceral branches (Fig. 1). The distal bend of the catheter should therefore be made sharper for the superior mesenteric than for the coeliac artery. Both of these vessels always branch off ventrally from the abdominal aorta, the distance between the openings measuring 0.5 to 2 cm (CAULDWELL & ANSON). Since the superior mesenteric artery lies caudal to the coeliac artery, the movements of the catheter tip along the ventral aortic wall need to be directed slightly more caudally for the former vessel. The movement should therefore be started at the level of the middle part of the second lumbar vertebra (Fig. 2).

When the catheterizing movements are directed cranially, the tip of the catheter meets the opening of the superior mesenteric artery first. If, on the other hand, the catheter is directed from above, past the openings of the coeliac and superior mesenteric arteries, the tip of the catheter is seldom caught up. Only when the tip of the catheter hugs the wall of the aorta, due to the aid of a guide-wire, can the catheter sometimes be led into the coeliac artery (ÖDMAN), although never into the superior mesenteric artery.

The openings of the visceral arteries often lie close to one another, and in consequence the catheter tip is sometimes by mistake passed into the wrong branch. When an attempt is being made to catheterize the superior mesenteric artery there is always a risk that the tip of the catheter will slip

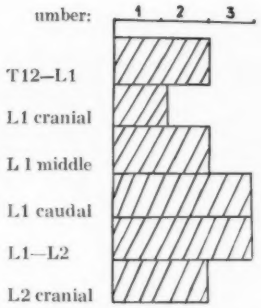

Fig. 2. Site of origin of superior mesenteric artery in relation to spinal column, evaluated in 13 angiographic examinations of branches of abdominal aorta.

into a renal artery. The coeliac artery, on the other hand, may usually be avoided. Fluoroscopy is often of assistance in indicating which branch has been catheterized. When the catheter enters a renal artery, it swerves off dorsally and laterally, even if at first it sometimes lies a fair distance ventral to the aorta (Fig. 1). When in the superior mesenteric artery, it takes the form of a long U-shaped bend in the sagittal plane, with the extremity directed caudally, when in the coeliac artery, it points ventrocaudally. The catheter may be pushed into the latter branch for a distance of 5 to 6 cm at the most; it penetrates much farther into the superior mesenteric artery (ÖDMAN).

If fluoroscopy gives no definite information as to which branch has been catheterized, the exact position of the catheter tip may be determined by a preliminary manual injection of 10 to 15 ml of a 45 % contrast medium. (Urografin — Schering — was used in these studies.) A lower concentration should not be employed. With a 45 per cent solution, or higher, the patient experiences the injection as a sensation of warmth, the site of which varies according to the branch into which the solution has flowed — if into the superior mesenteric artery, warmth is experienced in the pit of the stomach or sometimes throughout the whole abdomen. It is thus possible to obtain information concerning the position of the tip of the catheter even before the test film is ready.

Even if the fluoroscopic findings indicate that the catheter is in the superior mesenteric artery it is advisable to carry out a preliminary injection before the actual angiographic procedure, since the former will reveal whether the areas of diagnostic interest have actually been filled or not. It will also demonstrate whether the contrast medium, on account of vascular anomalies or because the catheter tip has been pushed too far in a peripheral direction, has become concentrated to one limited section of the superior mesenteric system. The latter situation should not be allowed to persist during the actual angiographic examination in which larger doses of contrast medium are used.

For the angiographic examination, 0.8 to 0.9 ml Urografin 45 % per kg of bodyweight should be injected at a rate of 8 to 9 ml per second. Manual injection is hardly capable of producing such a large flow of contrast medium. An injector apparatus should therefore be used. The passage of the solution through the different parts of the vascular system is recorded by means of multiple bi-plane exposures.

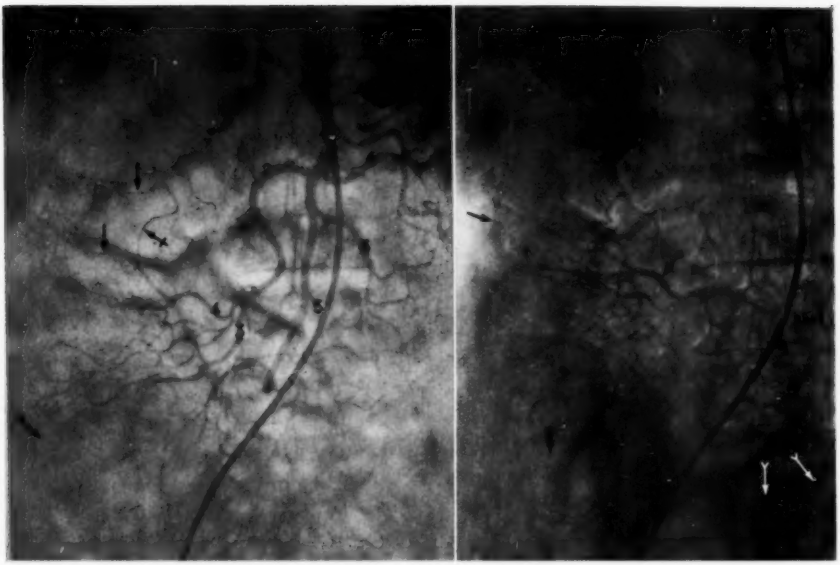

a b

Fig. 3. Cancer of caecum (verified at operation). a) Arterial phase. Tip of catheter in superior mesenteric artery. Middle colic artery (1); ileo-colic artery (2) with ileal branch (3) and colic branch (4); ileal arteries (5) and jejunal arteries (6). Colon arteries (→) with longitudinal anastomoses (↔). No arteries in cancerous area (›→). b) Parenchymatous and venous phase. Colon wall (→) with demarcation line (↔) indicates cancerous area, which is not filled with contrast medium. Wall of small intestine (›→). Mesenteric vein (○→).

Not only the superior mesenteric artery and its branches (Fig. 3 a) but also the intestinal wall and the venous return flow (Fig. 3 b) may be demonstrated with this technique. In normal subjects a typical vascular pattern may be seen in the colon, the main components of which are transverse, slightly tortuous arcades, approximately 2 mm thick, with scanty ramifications. Longitudinal communications may, however, sometimes be seen between them. When the haustrations are distinguishable in the parenchymal phase, the arcades are often seen to be running in their recesses. The contrast medium seems in this phase to be concentrated in the innermost layer of the colon wall, with the result that the outline of the mucous membrane is demonstrated. Multiple, millimeter-wide, profusely ramified arteries are seen in the walls of the small intestine (Fig. 4). The wall is seen as a millimeter-thick layer, which probably represents the mucous membrane (Fig. 3 b). The outlined arcades and mucous membrane in both the large and small intestine change in appearance according to the degree of intestinal distention and the digestive phase.

Fig. 4. Multiple slender, profusely branching arteries in wall of small intestine (→). Displacement to right due to splenic enlargement. Aberrant liver artery (↔).

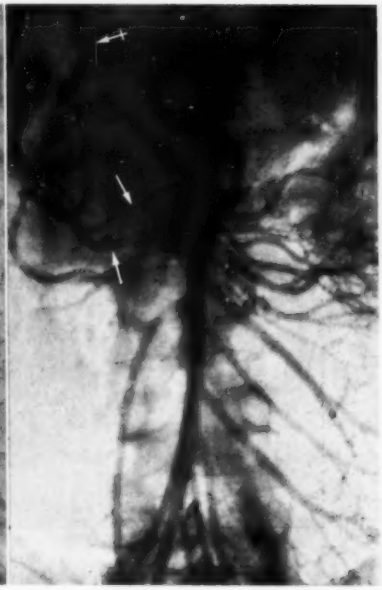

Fig. 5. Filled pancreatico-duodenal arcades (→) and liver arteries. Note straight outline (↔), corresponding to site where hepatic artery divides.

Vessels normally belonging to the coeliac system often become filled with contrast medium. Aberrant liver arteries arising close to the origin of the superior mesenteric are sometimes filled, as are omental arteries and the arcade of the greater curvature of the stomach. Contrast medium may also flow through the pancreatico-duodenal arcades to the gastroduodenal artery (Fig. 5), and occasionally from there out into the liver arteries.

The following information was obtained from the pathologic cases examined.

Expansive processes caused displacement in various directions (Fig. 4). In connection with metastases in the mesenteric lymph glands the arteries in that region were stretched, spread out, and sparse. Carcinoma of the colon manifested itself as an avascular area clearly delimited from the surroundings; no contrast medium was seen in the mucous membrane of the affected area (Fig. 3). This is not in agreement with the findings of SCHOBINGER et coll. In a case of cirrhosis of the liver and ulcerative colitis, the superior mesenteric artery and its branches were widened.

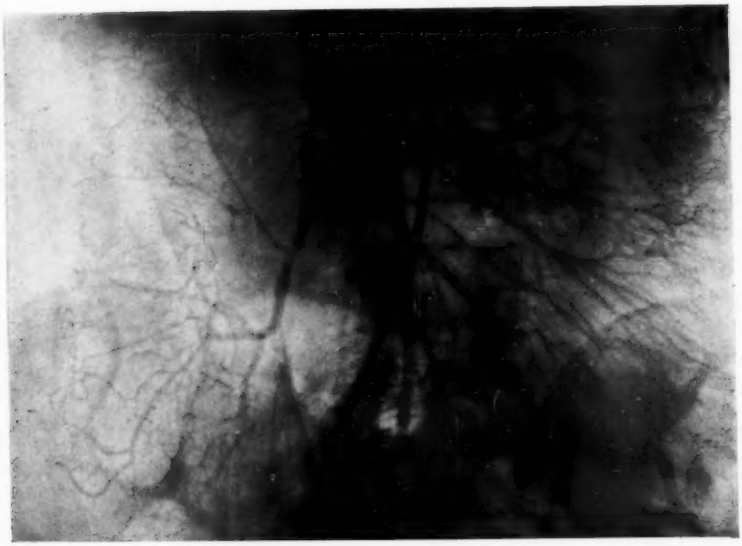

a

b

Fig. 6. Cirrhosis of liver and ulcerative colitis.

a) Superior mesenteric artery with widened branches, particularly ileo-colic artery (→). Usual arcade pattern absent in ascending colon.

b) Abundance of irregular, tortuous veins in and around thickened colon wall, emptying into a large mesenteric vein (→).

The vascular arcades in the colon were irregular and wide, and the outlined wall thicker than normal. The veins became filled unusually early in relation to the arteries, and in the colon wall or its neighbourhood there were clumps of varicose veins which emptied into the superior

mesenteric vein through widened branches (Fig. 6). The changes were attributable to the liver cirrhosis and/or ulcerative colitis. In the former condition, widening and varicose alteration of the veins may occur, and occasionally a wide superior mesenteric artery has been demonstrated by aortography (NELSON). On the other hand, arteriovenous shunts in the intestinal wall, which may give rise to the vascular changes in question, may be present in ulcerative colitis.

Discussion

Selective angiography of the superior mesenteric artery has previously been mentioned by BIERMAN et coll. and MORINO et coll. in connection with reports on catheterization of the visceral branches of the abdominal aorta. These authors used the Cournand instrument, which cannot be introduced percutaneously into the blood vessels, nor permanently bent like a radiopaque polythene catheter. The instrument was introduced by way of an artery (radial, humeral, or brachial) in the left arm in their investigations; the path to the superior mesenteric was hence long, and led past some difficult bends. It is especially troublesome to direct the catheter from the left subclavian artery through the aortic arch to the descending aorta, as the tip tends to slip down into the ascending aorta. This method of catheterization thus seems to be much more complicated than the one now described. Furthermore, with the antegrade technique only relatively narrow arteries can be selected, and it is therefore not possible to use catheters of as large a calibre as that employed in the present investigation. The difficulty of manoeuvring the catheter tip from the abdominal aorta out into the superior mesenteric artery was not encountered with retrograde catheterization. In point of fact, this vessel seemed to be the lumbar aortic branch most easily accessible with the technique in question.

Since the superior mesenteric system has proved to be sensitive to contrast medium when examined by lumbar aortography (GOTTLOB, MCAFEE, and VÖLPEL) the question of complications was given special attention in the present study. No untoward effects of any kind were noted, however. It is true that my experience of the actual angiographic procedure is limited, seeing that only ten complete examinations have been carried out, but on the other hand a total of twenty-seven test examinations of the superior mesenteric artery have been performed without any ill-effects in connection with angiography of the coeliac artery, using 15 to 20 ml of Urografin 45 % or 60 %. Nor, as far as I am aware, has any damage been caused to the superior mesenteric system by lumbar aortography with Urografin.

SUMMARY

The technique for percutaneous selective angiography of the superior mesenteric artery is described. It is based on the use of a pre-modelled radiopaque polythene catheter which is introduced transfemorally. The advantages of the method as compared with antegrade catheterization of the superior mesenteric with the Cournand-catheter are discussed and the possibility of damage due to the contrast medium is considered.

ZUSAMMENFASSUNG

Die Technik bei der perkutanen selektiven Angiographie der Arteria mesenterica superior wird beschrieben. Sie ist auf der Anwendung eines geformten röntgendichten Polythenkatheters basiert, der transfemoral eingeführt wird. Die Vorteile dieser Methode im Vergleich mit der antegraden Katheterisierung der Mesenterica superior mit dem Cournandkatheter werden besprochen. Die Möglichkeiten einer Schädigung durch das Kontrastmittel wird erwähnt.

RÉSUMÉ

L'auteur décrit la technique de l'angiographie sélective percutanée de l'artère mésentérique supérieure. Elle est basée sur l'emploi d'un cathéter en polythène radio-opaque à laquelle on donne à l'avance la courbure voulue et qu'on introduit par l'artère fémorale. L'auteur examine les avantages de cette méthode par rapport au cathétérisme antérograde de l'artère mésentérique supérieure avec la sonde de Cournand et envisage la possibilité d'incidents dus au moyen de contraste.

REFERENCES

Bierman, H. R., Miller, E. R., Byron Jr, R. L., et coll.: Intra-arterial catheterization of viscera in man. Amer. J. Roentgenol. 66 (1951), 555.

Cauldwell, E. W. and Anson, B. J.: The visceral branches of the abdominal aorta: Topographical relationships. Amer. J. Anat. 73 (1943), 27.

Gottlob, R.: Angiographie und Klinik. Wilhelm Maudrich, Wien-Bonn 1956.

McAfee, J. G.: Survey of complications of abdominal aortography. Radiology 68 (1957). 825.

Morino, F., Tarquini, A. & Olivero, S.: Artériographie abdominale sélective par le cathétérisme de l'artère humérale. Presse méd. 64 (1956), 1944.

Nelson, O. A.: Arteriography in diagnosis of upper abdominal conditions. Northw. Med. 44 (1945), 314.

Odén, B. O. and Wallensten, S.: Mesenteric vascular occlusion. Acta chir. Scand. 110 (1955—1956), 177.

Ödman, P.: Percutaneous selective angiography of the coeliac artery. Acta radiol. (1958) Suppl. 159.

Schobinger, R., Blachman, C. and Kan Lin, R.: Operative intestinal arteriography. Acta radiol. 48 (1957), 330.

Seldinger, S. I.: Catheter replacement of the needle in percutaneous arteriography. Acta radiol. 39 (1953), 368.

Völpel, H. W.: Die Indikation der Aortographie. Verh. dtsch. Ges. KreislForsch. 17 (1951), 305.

AUS DER CHIRURGISCHEN UNIVERSITÄTSKLINIK (DIREKTOR: PROF. DR. R. ZENKER), MARBURG/LAHN, WEST-DEUTSCHLAND

NORMALE UND PATHOLOGISCHE LUNGENSEGMENTE IM SELEKTIVEN ANGIOGRAMM

von

Hh. Löhr, H. Scholtze und *W. Grill*

Seit über 25 Jahren bemüht man sich, die Lungengefässe durch Kontrastmittelinjektion sichtbar zu machen, um die Veränderungen des Lungengefässbaumes in morphologischer und funktioneller Hinsicht für die Diagnostik der Lungenerkrankungen auszuwerten. Zunächst versuchte man, die Lungengefässe während der Endphase der Angiocardiographie durch Serienaufnahmen darzustellen (ROBB und STEINBERG. DOTTER und STEINBERG). Wertvolle Beiträge zum Studium der Gefässveränderungen hauptsächlich beim Bronchialkarzinom und bei der Lungentuberkulose stammen von DE CARVALHO, AMEUILLE u. Mitarb., ANDERSEN u. Mitarb., und von RIMINI u. RODRIGUEZ, u. a.

Die Bilder der 'Angiopneumographie', der Gesamtdarstellung der Lungengefässe sind wegen der verwirrenden Überlagerung der Pulmonalisäste schwer zu deuten. Die moderne Lungenchirurgie fordert aber nicht nur eine möglichst weitgehende Röntgendiagnostik der Parenchymveränderungen, sondern auch ihre exakte Lokalisation innerhalb eines bestimmten Segmentes, nachdem das Lungensegment als funktionelle und chirurgische Einheit immer mehr in den Vordergrund des Interesses

Bei der Redaktion am 14. Januar 1958 eingegangen.

gerückt ist. Die genaue Segmentlokalisation erweist sich mit der Angiopneumographie als sehr schwierig, selbst wenn man simultane Serienaufnahmen in 2 Ebenen anfertigen kann. Ausserdem kommt das Kontrastmittel trotz Verwendung grösserer Mengen nur stark verdünnt im Ausbreitungsgebiet der Lungenarterie an, sodass die Kontraste leiden und eine ins Einzelne gehende Beurteilung der Gefässveränderungen unmöglich wird. Etwa zur gleichen Zeit versuchte man deshalb, das Kontrastmittel durch einen in das rechte Herz eingeführten Katheter in den Stamm der Lungenarterie zu injizieren, nachdem FORSSMANN 1929 den Weg dazu gewiesen hatte. Besonders zu erwähnen sind in diesem Zusammenhang die Untersuchungen von JÖNSON, BRODÉN und KARNELL, und LÖFFLER. Aber auch diese Methode lässt keine ganz exakte Darstellung der Lungengefässveränderungen zu.

Um die Ausarbeitung der 'selektiven Lungenangiographie', die alle diese Nachteile vermeidet und ihre Einführung in die Diagnostik der Lungenkrankheiten haben sich FORSSMANN und der Kölner Arbeitskreis um KNIPPING (BOLT u. Mitarb. 1957), u. a. grosse Verdienste erworben. Die Katheterspitze wird bei dieser Methode bis in die Lungensegmentarterien vorgeführt. Die genannten Autoren haben gezeigt, dass die selektive Angiographie mit Hilfe des Herzkatheters die einzelnen Segmentarterien klar und deutlich hervortreten lässt und dass mit ihrer Hilfe wertvolle Schlüsse für die Diagnostik der verschiedensten Herz- und Lungenerkrankungen möglich sind. Das Verfahren hat den Vorteil, dass man vor der Ausführung von Lungenresektionen besonders interessierende Teilabschnitte der Lunge systematisch und gezielt darstellen kann. Voraussetzung ist die Kenntnis der Segmentanatomie der Lunge und die Beherrschung einer subtilen Technik, um die Katheterspitze in die bestimmte Lungensegmentarterie einführen zu können, was bei manchen Erkrankungen, z. B. bei fortgeschrittenen Fällen von Lungentuberkulose mit vielfachen Verziehungen der Lungenarterie durch schrumpfende Parenchymprozesse, Pleuraschwarten und Kollapsmassnahmen nicht immer leicht ist.

Die Kölner Schule um KNIPPING bemühte sich, aufbauend auf den fundamentalen Untersuchungen von COURNAND und seiner Schule, in Zusammenarbeit mit FORSSMANN vor allem um die Klärung pathophysiologischer Zusammenhänge zwischen Herz- und Lungenerkrankungen. RINK (BOLT u. Mitarb. 1957) zeigte an Hand eines grösseren Tuberkulosekrankengutes die vielseitigen Veränderungen der Lungengefässe im selektiven Angiogramm, um Hinweise für die Indikationsstellung zu den Teilresektionsverfahren an der Lunge zu gewinnen. In einer Monographie fassten BOLT, FORSSMANN und RINK (1957) ihre Erfahrung an 2.000 selektiven Lungenangiographien zusammen. Weitere wichtige Arbeiten stammen von CICERO und CASTILLO in Mexico.

Eine eingehende Monographie erschien 1954 von NORDENSTRÖM, der die experimentellen Grundlagen zur temporären Blockierung der Lungenarterie einer Seite mit Hilfe eines Ballon-Katheters mit doppeltem Lumen schuf. Diese Methode ermöglicht es, den Gefässbaum eines ganzen Lungenflügels mit geringsten Mengen von Kontrastmittel darzustellen und die Einzelheiten der Gefässveränderungen während der Durchleuchtung in aller Ruhe durch Zielaufnahmen festzuhalten, da die Strömungsgeschwindigkeit in der blockierten Lunge stark verlangsamt ist. Durch die Kontrastmittelinjektion distal von der blockierten Lungenarterie gelingt es, nicht nur die Lungenarterie, sondern auch die Lungenvenen selektiv darzustellen. Durch densigraphische Messungen der Durchblutung des Lungengewebes vor und nach der Blockierung konnte gezeigt werden, dass der Blutgehalt der verschlossenen Lunge beträchtlich abfällt, während der Blutgehalt der nicht blockierten Lunge etwa um 1/3 zunimmt. Allgemeinwirkungen auf den Organismus konnten durch ausgedehnte experimentelle Untersuchungen ausgeschlossen werden. NORDENSTRÖM konnte auch röntgenologisch eine Kommunikation zwischen dem Bronchial- und dem Lungengefässsystem am lebenden Hund nachweisen. Wahrscheinlich ist die Tatsache, dass das Kontrastmittel nach der Injektion bei verschlossener Lungenarterie zwar langsam fliesst, aber mit der Zeit doch verschwindet, durch das Funktionieren solcher Anastomosen zwischen dem Bronchial- und dem Lungengefässsystem zu erklären.

Obwohl die Kontrastdarstellung der Lungengefässe nach den Untersuchungen von VIETEN und SCHOENMACKERS an postmortalen Angiogrammen eine Differentialdiagnose nicht erlaubt, so wünschenswert dies auch wäre, ist die besondere Bedeutung der Lungenangiographie in folgenden Tatsachen zu sehen:

1. Sie erlaubt eine genaue Lokalisation einer Veränderung innerhalb eines bestimmten Segmentes, was besonders im Hinblick auf die geplante Lappen- oder Segmentresektion sehr wichtig ist.

2. Sie gestattet es, aus den morphologischen Veränderungen des einzelnen Segmentes geradezu die pathophysiologischen Veränderungen eines solchen begrenzten Lungenteiles abzulesen, lange bevor die funktionelle Schädigung in den Ergebnissen der üblichen physiologischen Funktionsproben zum Ausdruck kommt.

Die Untersuchung des Gasstoffwechsels und der Blutgasanalyse können nur summarische Urteile über beide Lungenflügel, in speziellen Fällen über einen ganzen Lungenflügel abgeben.

Einen genauen Einblick in die Morphologie und Funktion eines einzelnen Segmentes erlaubt bisher nur die selektive Lungenangiographie. Einen besonderen Vorteil dieses Verfahrens gegenüber der gezielten Bronchographie sehen wir darin, dass bei der Lungenangiographie das Kapillargebiet von dem Kontrastmittel durchflossen wird und das die feinsten,

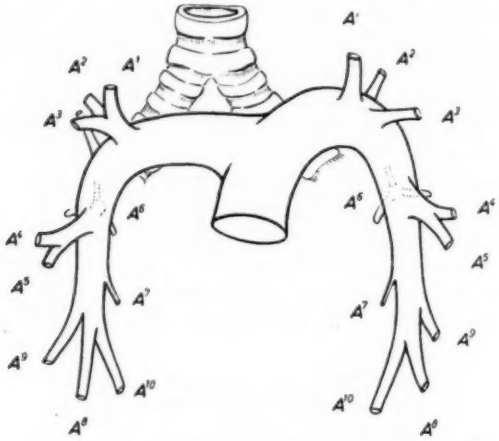

Abb. 1. Schematische Abbildung der normalen Abgänge der Segmentarterien.

dem Kapillarkreislauf unmittelbar vorgeschalteten kleinen Arterien, die für die Beurteilung der Funktion sehr wichtig sind, noch abgebildet werden, während man bei der Bronchographie durch absichtliche Erhöhung der Viskosität des Kontrastmittels eine Alveolarfüllung unter allen Umständen zu vermeiden sucht.

Die Retention des viskösen Kontrastmittels in den Alveolen kann unerwünschte Folgen haben. Der Durchmesser der kleinsten Bronchen, deren Abbildung bei der Bronchographie gerade noch zugelassen wird, liegt etwa in einer Grössenordnung von 1 mm (VIETEN), während bei der Angiographie die kleinsten, im Röntgenbild noch erkennbaren Arterien des Lungenmantels etwa 150 μ gross sind. In diesem Unterschied ist eine beträchtliche Verfeinerung vor allem der funktionellen Diagnostik gegenüber der Bronchographie begründet.

Material und Methoden

Der Arbeit liegen Erfahrungen an 250 Kranken mit den verschiedensten Lungenerkrankungen zu Grunde, die im Rahmen der präoperativen Diagnostik mit Hilfe der selektiven Lungenangiographie untersucht wurden. Von diesen Kranken stehen uns zur Beurteilung und Ergänzung der Lungenangiogramme die während der stationären Beobachtung erhobenen klinischen und röntgenologischen Befunde zur Verfügung. Ausserdem liegen die Ergebnisse der lungenphysiologischen Untersuchungen (Spirometrie, Blutgasanalyse, Druckmessungen im kleinen Kreislauf) vor. 84 Kranke wurden einer Lungenresektion (Pneumonektomie, Lobektomie oder Segmentresektion, z. T. in Kom-

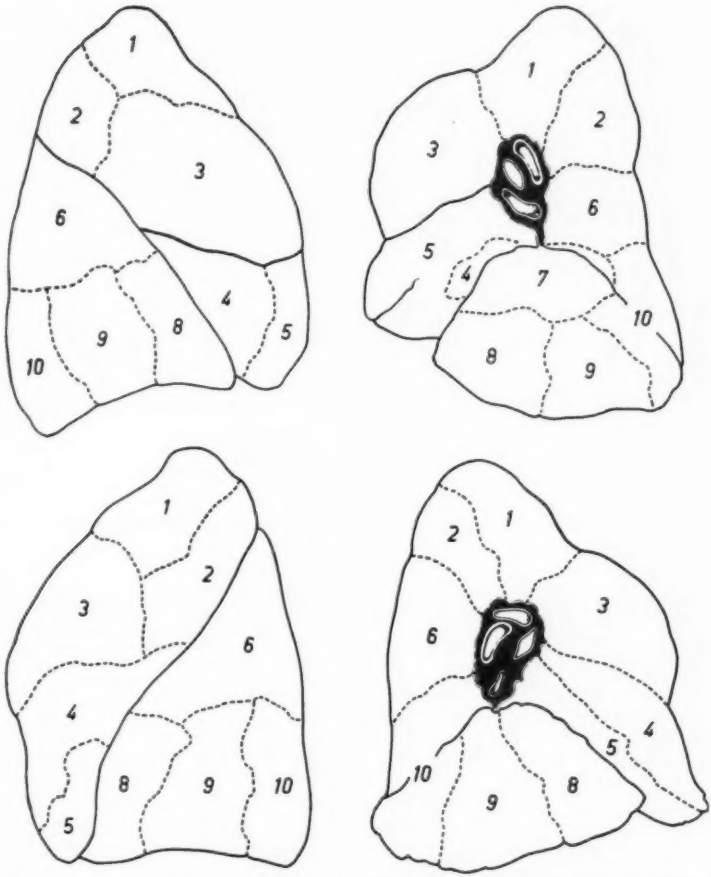

Abb. 2. Grenzen der normalen bronchopulmonalen Segmente auf der Pleuraoberfläche. Internationale Nummerierung. *Oben:* Rechte Lunge von lateral und mediastinal. *Unten:* Linke Lunge von lateral und mediastinal.

bination oder bilateral) unterzogen, sodass es uns möglich war, die während des Eingriffes erhobenen Befunde am ganzen Lungenflügel, die Ergebnisse der makroskopischen und mikroskopischen Untersuchungen der Operationspräparate und z. T. auch die Röntgenaufnahmen der mit Kontrastmittel injizierten Präparate mit den Angiogrammen zu vergleichen.

Technik. Die Untersuchung wird in gleicher Weise wie die Katheterisierung des Herzens bei angeborenen und erworbenen Herzfehlern mit Hilfe eines Cournand-Katheters verschiedener Grösse in Lokalanästhesie ausgeführt. Man lässt die gebogene

Katheterspitze unter Rotation des Katheters um die eigene Achse unter Durchleuchtungskontrolle durch das rechte Herz hindurch in die rechte oder linke Lungenarterie, von da in die gewählte Segmentarterie hineingleiten. Als Kontrastmittel dient 76 %-iges Urografin (Schering, Berlin).

Gleichzeitig mit der Injektion von 8 bis 10 bis 12 ml Kontrastmittel belichtet man die Aufnahme in verschiedenen Ebenen am Durchleuchtungsgerät. Um Reizleitungsstörungen des Herzens durch die Manipulationen mit dem Katheter sofort erkennen zu können, verfolgen wir das EKG laufend am Sichtgerät und schreiben es sofort mit einem Direktschreiber auf, sobald Reizleitungsstörungen auftreten. Auf diese Weise kann man die Art der Reizleitungsstörung schnell erkennen und u. U. eine geeignete Behandlung einleiten.

Die Gefahr der Reizleitungsstörungen durch die Katheterspitze ist aber bei herzgesunden Kranken bei weitem nicht so gross wie beim Herzkranken. Gute Erfahrungen haben wir mit Hartstrahlaufnahmen und Feinstfokus gemacht. Man erhält so kürzeste Belichtungszeiten und die Gefässzeichnung ist auf diesen Bildern viel schärfer als mit der normalen Technik. Zum Teil konnten wir die Aufnahmen am Seriengerät nach JANKER unter simultaner Schaltung der a. p. und seitlichen Aufnahmen ausführen.

Den Abschluss der Untersuchung bildet die Druckmessung in den einzelnen Abschnitten der Lungenarterie und des rechten Herzens mit dem Kompensatormanometer nach HANSEN und dem Druckmessgerät nach NEUHAUS.

Verwendet wurde die der internationalen Nomenklatur des Bronchialsystems angepasste Benennung der Lungengefässe, die wir in unserer Monographie über die Lungenresektionen (1954) erläutert haben. Abb. 1 gibt einen schematischen Überblick über die Abgänge der einzelnen Segmentarterien. Die Katheterspitze wird bei der selektiven Darstellung in die Ostien der Segmentarterien eingelegt.

Die Nomenklatur des linken Lungenflügels ist im wesentlichen die gleiche wie rechts, abgesehen davon, dass die Lingula als Homologon des rechten Mittellappens ein Teil des Oberlappens ist und dass auf der linken Seite ein medio-basales Segment S^7 nur in den wenigsten Fällen deutlicher ausgeprägt ist, weshalb es in die internationale Nomenklatur nicht aufgenommen wurde.

Da im morphologischen Bild des Segmentangiogrammes auch die feinsten, eben beginnenden Schädigungen des Lungenparenchymas zum Ausdruck kommen, muss man sich eine genaue Vorstellung über die angiographische Gestalt der normalen Segmentarterie verschaffen, um pathologische Veränderungen genauer beurteilen zu können. Die normale Anatomie der Segmentgefässe mit ihren mannigfachen anatomischen Varianten wurde von BOYDEN am anatomischen Präparat und von HORNYKIEWYTSCH und STENDER im Schichtbild ausführlich dargestellt. Mit dem Erscheinungsbild der Segmentbronchen und ihren Varianten im Bronchogramm befassten sich STUTZ und VIETEN in einer ausführlichen Monographie. Es sollen deshalb nur die wichtigsten, für das Verständnis nötigen Tatsachen aufgeführt werden. Die Grenzen der Lungensegmente auf der Pleuraoberfläche, wie wir sie in Zusammenarbeit mit HEBERER bei der anatomischen Präparation von 200 Lungenpräparaten durch Injektion von verschiedenfarbigem Agar-Agar vom Segmentbronchus aus als häufigste Anordnung fanden, zeigten die Abb. 2. Die Untereinheiten der Lungenlappen können für sich getrennt reseziert werden, wie unsere eigenen Erfahrungen (ZENKER und HEBERER) gezeigt haben.

A. Normale Anatomie der Segmentarterien bei Angiographie

1. Die Arterien des rechten Oberlappens. Die 3 Segmentarterien des rechten Oberlappens sind: die apikale Segmentarterie A^1 (Abb. 3), die posteriore Segmentarterie A^2 (Abb. 4) und die anteriore Segmentarterie

Abb. 3 A^1, Segmentarterie des apikalen Segmentes S^1 des rechten Oberlappens. Venöser Rückfluss über die V. apicalis V^1.

Abb. 4. A^2, Segmentarterie des posterioren Segmentes S^2 des rechten Oberlappens.

Abb. 5. A^3, Segmentarterie des anterioren Segmentes S^3 des rechten Oberlappens. Angedeutet sind die Abgänge von A^1 und A^2.

A^3 (Abb. 5). In der Regel bildet die Arterie zum rechten Oberlappen eine Bifurkation mit den Ästen A^{1+2} und A^3. In etwa 1/5 der Fälle besteht eine Trifurkation (Abb. 5), bei der A^2 oder Teile von A^1 oder A^3 den mittleren Ast darstellen.

A^1 entspringt vom obersten medialen Rand der Oberlappenarterie, zieht in latero-dorsaler und cranialer Richtung zur Lungenspitze und versorgt die Lungenspitze und die subapikalen vorderen und mediastinalen Teile des Oberlappens bis in Höhe der 2. Rippe vorne (apikales Segment S^1).

Ursprung und Verlauf von A^2 wechseln sehr. A^2 kommt als einzelner Stamm nur in etwa 1/3 aller Fälle vor (Abb. 4). Sie entspringt dann entweder an der Hilusvorderseite von der Oberlappenarterie oder an der Interlobärseite von der Pars interlobaris der Lungenarterie. In etwa 2/3 der Fälle ist A^2 durch 2 oder mehrere Äste dargestellt, die dann entweder von A^1, A^3 oder A^6, meist von der Hilusvorderseite und der Interlobärseite des Oberlappens gleichzeitig entspringen. A^2 zieht in der Regel bogenförmig in dorsaler, cranialer und etwas lateraler Richtung und versorgt den hinteren und basalen, subapikalen Teil des Oberlappens (posteriores Segment S^2).

A^3 entspringt etwa in der Hälfte der Fälle von der Oberlappenarterie als selbständiger Ast an der Vorderseite des Hilus (Abb. 5), in der anderen Hälfte der Fälle entspringt ein Subsegmentast von vorne, der andere von der Interlobärseite. Ein Subsegmentast verläuft horizontal in late-

Abb. 6. Segmentarterien A^4 und A^5 des rechten Mittellappens (S^{4+5}).

Abb. 7. A^6, Segmentarterie des apikalen Unterlappensegmentes S^6 des rechten Unterlappens.

raler Richtung, der andere in fast sagittaler Richtung. Ihr Versorgungsgebiet, das anteriore Segment S^3, nimmt die vorderen, seitlichen und unteren Teile des Oberlappens ein.

2. Die Arterien des rechten Mittellappens. Die beiden Segmentarterien des Mittellappens, A^4 für das laterale Segment S^4 und A^5 für das mediale Segment S^5, entspringen in über der Hälfte der Fälle von einem kurzen gemeinsamen Stamm, der seinen Abgang von der Vorderseite der Pars interlobaris der Lungenarterie in der Interlobärfissur nimmt (Abb. 6). In den übrigen Fällen finden sich 2 getrennte, von der Lungenarterie abgehende Äste, die dann aber meist nicht die entsprechenden bronchopulmonalen Segmente versorgen, sondern teilweise auf das benachbarte Segment übergreifen. Im allgemeinen kann man sagen, dass A^4 die seitlichen hinteren Teile, A^5 die vorderen medialen Teile des Mittellappens versorgt.

3. Die Arterien des rechten Unterlappens. S^6, das apikale Segment des Unterlappens, sitzt der basalen Segmentgruppe wie eine Kappe auf und nimmt dem Volumen nach etwa die Hälfte des ganzen Lappens ein.

A^6 (Abb. 7) zeigt im Angiogramm ein sternförmiges Ausbreitungsgebiet dicht neben dem rechten Herzrand etwa in Höhe der Einmündungsstelle der V. cava superior. A^6 entspringt in Höhe des Abganges der

Abb. 8. Segmentarterien A^8, A^9 und A^{10} der basalen Segmentgruppe des rechten Unterlappens.

Abb. 9. A^4 und A^5, Segmentarterien der Lingula S^{4+5} des linken Oberlappens.

Mittellappenarterie oder etwas unterhalb davon und zieht nach dorsal. In 4/5 der Fälle versorgt eine einzige Arterie A^6 das Segment, d. h. A^6 geht als kurzer gemeinsamer Stamm von der Unterlappenarterie ab, um sich dann in ihre 3 Subsegmentäste aufzuspalten. In den übrigen Fällen findet man eine strauchartige Aufzweigung, wobei die einzelnen Äste von den verschiedensten Stellen der Pars basalis der Lungenarterie entspringen können.

Die Arterien der basalen Segmentgruppe des rechten Unterlappens (Abb. 8) entspringen von einem kurzen gemeinsamen Stamm, der Pars basalis der Lungenarterie, um sich in Form eines Dreifusses aufzuspalten. A^{10}, die kräftigste Arterie zum postero-basalen Segment S^{10}, liegt am weitesten medial und dorsal, A^9, die Arterie des latero-basalen Segmentes S^9, am weitesten lateral. Zwischen beiden Arterien verläuft A^8, die Arterie zum antero-basalen Segment, nach vorne. A^7, die Arterie des kleinen medio-basalen Segmentes S^7, entspringt etwas höher am medialen Rand der Pars basalis. Schon diese wenigen Aufnahmen zeigen den ausserordentlichen Formenreichtum der einzelnen Segmente.

4. Die Arterien des linken Oberlappens. Auf der linken Seite ist die Anordnung der Segmentarterien des Oberlappens durch die Erscheinung, dass die Lungenarterie über den Oberlappenbronchus hinwegzieht, grund-

sätzlich gegenüber der rechten Seite verändert. Meist sind mehr Arterien ausgebildet, als der Zahl der Segmente entspricht, da das anteriore Segment S^3 und die Lingulasegmente durch Arterien von der mediastinalen und der interlobären Seite des Lappens gleichzeitig versorgt werden. Ausserdem erhalten das apikale Segment S^1 und das posteriore Segment S^2 fast immer getrennte Arterien.

Die Bildung gemeinsamer Stämme erfolgt von zwei zentralen Punkten aus: die erste Gruppe entspringt von der Pars anterior der A. pulmonalis an der Vorderseite des Lungenhilus (A^1, Teile von A^2 und A^3, Varianten von A^4 und A^5). Die zweite Gruppe entspringt in der Interlobärfissur von der Pars interlobaris der Lungenarterie (Teile von A^1, A^2, A^{4+5}). Deshalb erhält man bei der Angiographie die verschiedensten Bilder. In der Regel sind die vom obersten Bogen der A. pulmonalis entspringenden Gefässe A^1, A^2 und A^{3b}.

A^2, die Arterie zum posterioren Segment S^2, ist daran zu erkennen, dass ihre äussersten Ausläufer im Gegensatz zu A^1 nicht bis zur Lungenspitze hinaufreichen. Die Versorgungsgebiete der 3 oberen Segmentarterien entsprechen im Allgemeinen der Anordnung auf der rechten Seite. Die Lingula besteht aus einem oberen Segment S^4 und einem unteren Segment S^5 (Abb. 9), da sie die Drehung, die der rechte Mittellappen bei seiner Spaltung vom Oberlappen ausführt, nicht mitmacht. Die entsprechenden Segmentarterien A^4 und A^5 entspringen in der Regel von einem kurzen gemeinsamen Stamm, der aus der Pars interlobaris der Lungenarterie hervorgeht. A^4 versorgt den oberen, ventralen, pericardialen und lateralen Teil der Lingula. A^5 breitet sich nach den unteren paracardialen Teilen und der Spitze der Lingula aus.

5. Die Arterien des linken Unterlappens. Die Anordnung der Arterien zum linken Unterlappen lässt gegenüber rechts keine grundsätzlichen Unterschiede erkennen. A^7 ist auf der linken Seite in nur etwa 10 % der Fälle deutlich ausgebildet. Sie entspringt dann meist von A^8.

6. Die Lungenvenen. Die Lungenvenen, die bei der Segmentresektion wegen ihrer meist intersegmentalen Lage als Wegweiser für die Spaltebene eine so grosse Rolle spielen (*e. g.* BOYDEN 1955) haben bei der selektiven Angiographie eine geringere diagnostische Bedeutung, da sie mit dem Katheter von dem rechten Herzen aus nicht unmittelbar erreichbar sind. Bei der Darstellung der kapillären Füllungsphase können sie jedoch abgebildet werden. Sie sind dann für die anatomische Zuordnung von Arterien zu einem bestimmten Segment eine willkommene Hilfe. Man schiebt dabei die Katheterspitze soweit in den Lungenmantel vor, dass sie das Lumen der Arterie fast ganz verschliesst und injiziert wenige milliliter Kontrastmittel vorsichtig unter mässigem Druck.

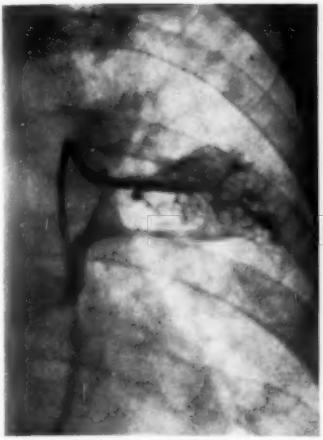

Abb. 10. Normales Subsegment von S^3 mit venösem Rückfluss über V^3 (Intersegmentvene S^3/Lingula).

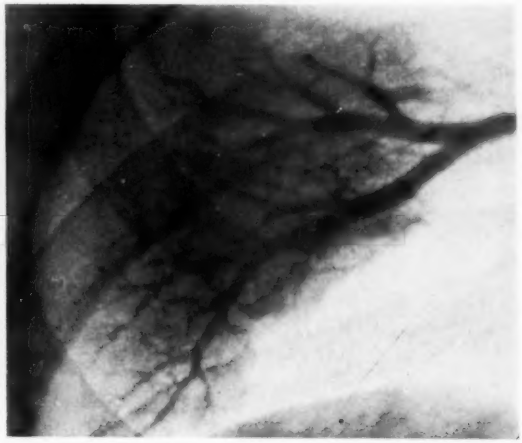

Abb. 11. Kapillarfüllung in normalem Lungengewebe (laterobasales Segment S^9 des rechten Unterlappens).

Abb. 3 zeigt die V. apicalis V^1 des rechten Oberlappens, dargestellt durch Injektion von A^1. In Abb. 10 hat sich die V. inferior V^3 abgebildet, die sich in der Intersegmentebene zwischen S^3/Lingula ausbreitet.

7. Die kapilläre Füllungsphase der normalen Lunge. Schiebt man die Katheterspitze soweit in den Lungenmantel vor, dass sie das Lumen der Arterie fast ganz verschliesst und injiziert man das Kontrastmittel ganz vorsichtig unter mässigem Druck, wie es in Abb. 11 geschehen ist, so erscheint für einen Augenblick ein dichter Kontrastmittelschleier um die feinsten Gefässabgänge herum, der mit grosser Geschwindigkeit über die zugeordneten Venen wieder abfliesst. Der ganze Vorgang dauert etwa 1 bis 2 Sekunden. Dieser Schleier entsteht beim Durchfluss des Kontrastmittels durch das Kapillargebiet der Alveolen. In dem Erscheinen des Phänomens sehen wir einen Beweis dafür, dass das Kapillar- und Alveolargebiet des Lungenmantels durch die Grundkrankheit nicht geschädigt oder zerstört wurde. In Abb. 12 bis 14, und 16 bis 18 sind Beispiele einer ausgedehnten Schädigung des Kapillargebietes wiedergegeben.

Wir haben uns die Frage vorgelegt, bis zu welcher Grössenordnung die Lungenarterien angiographisch darstellbar sind. Nach Messungen an unseren Röntgenbildern, auf denen kleinste Arterienverzweigungen in der Peripherie des Segmentes dargestellt sind, beträgt der Durchmesser einer solchen kleinsten, gerade noch erkennbaren Arterie etwa 1/5 mm. Der

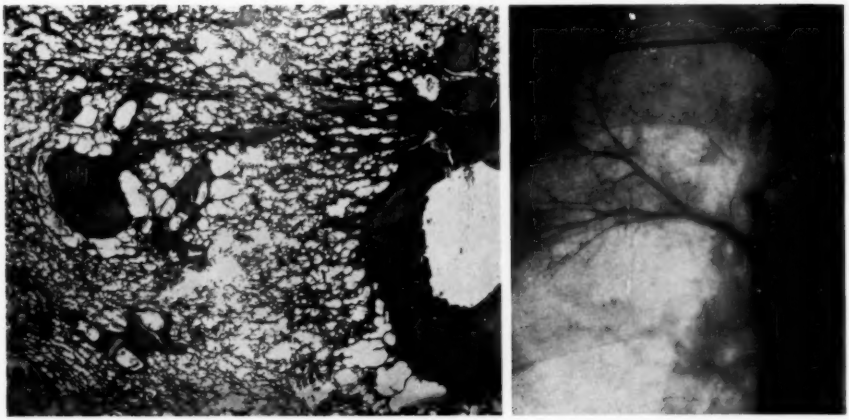

a b

Abb. 12. Spezifische Streuherde (a) verursachen im Angiogramm eine Rarefizierung (b) durch Einengung oder Verschluss der kleineren Gefässe.

Film-Focusabstand an unserem Durchleuchtungsgerät beträgt 70 cm. Wenn man als halben Thoraxdurchmesser des Patienten einen Betrag von 15 cm annimmt, so ergibt eine einfache Rechnung, dass ein Gefäss mit dem Durchmesser 0.2 mm im Röntgenbild in Wirklichkeit einen Durchmesser von 0.15 mm hat. Nach VON HAYEK liegt der Übergang von den kleinsten Lungenarterien zu den Arteriolen etwa bei einer Grenze von 50 μ. Man kann also sagen, dass man bei der angiographischen Darstellung der kleinsten Gefässabgänge des Segmentarterienbaumes ziemlich nahe an das Arteriolengebiet herankommt, dass man die Arteriolen und Kapillaren selbst aber nie einzeln abbilden kann. Sie ergeben aber als Summationseffekt den beschriebenen Kontrastmittelschleier um die kleinsten Arterienverzweigungen herum (Abb. 11).

Über das röntgenologische Erscheinungsbild einer normalen Segmentarterie kann man also folgendes zusammenfassen:

Die Segmentarterie besteht aus einem zentralen Hauptgefäss, von dem unter stetig abnehmenden Winkeln nach der Peripherie zu immer kleinere Seitenzweige bis zu den feinsten Verästelungen im Lungenmantel entspringen.

Das zentrale Hauptgefäss verläuft entsprechend der Lage des betreffenden Segmentes in einem natürlich geschwungenem Bogen unter kontinuierlicher Abnahme des Kalibers zur Peripherie in der Hauptachse des Segmentes.

Die Art der Aufzweigung der Gefässe lässt Vergleiche mit Verzweigungsarten im Pflanzenreich zu. Man unterscheidet den 'magistralen' oder 'dendroiden' Verzweigungstyp (magistralis = die Grundlage bildend, hauptsächlich. *Τὸ δένδρον* = der Baum) und den 'strauchartigen' oder 'thamnoiden' Verzweigungstyp (*ὁ θαμνος* = Strauch, Gebüsch, z. B. Abb. 7 und 15).

Zwischen diesen extremen Typen beobachtete VON HAYEK (1953) zahlreiche Übergangsformen der Aufzweigung der Segmentarterie. Die Aufzweigungswinkel projizieren sich je nach der Atemphase mit verschieden spitzen Winkeln auf die Filmebene. Die kleinsten, im Angiogramm erkennbaren Verzweigungen, die für die Beurteilung der Lungenfunktion so grosse Bedeutung haben, sind sicher noch Arterien, die dem Kapillarkreislauf aber unmittelbar vorgeschaltet sind. Die einzelnen Arteriolen und Kapillaren liegen jenseits der röntgenologischen Darstellbarkeit. Man kann aber das Kapillargebiet als wolkenartigen Schleier um die kleinsten Arterienverzweigungen herum sichtbar machen, wie es oben beschrieben wurde.

Die genannten Kennzeichen einer normalen Segmentarterie halten wir für besonders wichtig, um beurteilen zu können, ob in dem betreffenden Segment ein pathologischer Prozess vorliegt oder nicht.

B. Pathologie der Segmentarterien bei Angiographie

Die wichtigsten pathologischen Veränderungen des Segmentangiogramms bei den verschiedenen Lungenerkrankungen lassen sich auf Grund unserer Vergleichsuntersuchungen mit den nach der Lungenresektion gefundenen histologischen Veränderungen folgendermassen kurz zusammenfassen:

1. Kleine, über den Lungenlappen oder über einen ganzen Lungenflügel diffus ausgebreitete Streuherde spezifischer oder unspezifischer Genese verursachen in ihrer unmittelbaren Umgebung eine reaktive Fibrosierung der Gefässwand mit Verdickung hauptsächlich der Media und der Adventitia und Einengung oder Verschluss des Gefässes (Abb. 12 a). Am frühesten werden dabei zusammen mit dem Kapillargebiet die kleinsten, unmittelbar vorgeschalteten Arterien zerstört. Je weiter der Prozess fortschreitet, je enger die Streuherde zusammenrücken, um so grössere Arterien des Lungenmantels werden dabei betroffen. Diese Erscheinung zeigt sich im Segmentarteriogramm an einem mehr oder weniger starken Ausfall der kleinsten Seitenzweige des normalerweise reich verzweigten Segmentarterienbaumes (Rarefizierung Abb. 12 b). Ausserdem erleiden

Abb. 13. Rarefizierung und korkzieherartige Windung der Arterien des linken Unterlappens als Zeichen einer spezifischen Streuung unter einem Oleothorax.

Abb. 14. Vollständige Schrumpfung des rechten Oberlappens durch jahrelang bestehenden Kollaps mit schweren Zerstörungen des Gefässystems. Der rechte Oberlappen ist funktionell tot.

die kleinen Arterien in unmittelbarer Nähe der Streuherde infolge der lokalisierten Schrumpfung des Lungengewebes eine verschieden starke Verziehung, die sich im Angiogramm als korkzieherartige Windung des Gefässes mit sprungartiger Änderung des Kalibers zu erkennen gibt (Abb. 13).

Als sehr wertvoll für die Beurteilung der Ausdehnung des Prozesses und damit für die Operationsindikation hat sich uns die gezielte Lungenangiographie bei der Beurteilung von Bronchiektasen erwiesen. Manchmal ist man anhand des bronchographischen Befundes im Zweifel, wie weit benachbarte Segmente durch den Degenerationsprozess mitergriffen sind, und ob sie bei einer plurisegmentalen Resektion mitentfernt werden müssen, um ein Recidiv zu vermeiden. Oft zeigt dann das Angiogramm schon Gefässveränderungen in diesen Nachbarsegmenten infolge der den chronischen Entzündungsprozess der Bronchialwand begleitenden degenerativen Gefässveränderungen, obwohl eindeutige Bronchiektasen im Bronchogramm nicht sichtbar sind.

2. Die gleichen Erscheinungen der fibrösen Degeneration, der Gefässwandverdickung und des fortschreitenden Füllungsausfalles kleinster Seitenzweige der Segmentarterie beobachtet man bei jahrelang bestehender Funktionsschädigung des Lungengewebes unter Kollapsmassnah-

Abb. 15. Normales Gefässsystem (anteriores Segment S^3 des rechten Oberlappens) unter einem erst jüngst angelegten Pneumothorax wegen kavernösen Zerfalles im apiko-posterioren Segment S^{1+2} des rechten Oberlappens.

Abb. 16. Zerstörung des Parenchyms im anterioren Oberlappensegment S^3 links unter spezifischer Empyemresthöhle. Trotz Darstellung des venösen Rückflusses kommt keine kapilläre Füllung zustande.

Abb. 17. Rarefizierung, Spreizung und Engstellung als Zeichen eines Emphysem (mediales Subsegment von S rechts) durch schrumpfenden Prozess in der Lungenspitze.

men (Pneumothorax, Thorakoplastik, Pneumolyse, Oleothorax, Abb. 13) oder bei chronischer Atelektase.

Abb. 14 zeigt den durch eine chronische Atelektase völlig geschrumpften rechten Oberlappen mit seinen schwer geschädigten Gefässen. Abb. 15 zeigt dagegen, dass das Gefässsystem über einem erst vor kurzer Zeit angelegten Pneumothorax noch vollständig erhalten ist (A^3, Arterie des anterioren Oberlappensegmentes, rechts). Die jahrelang bestehende Minderdurchblutung und Minderbeatmung führt zu ausgedehnten reaktiven Gefässwandprozessen. Man kann also aus dem Grade der im Angiogramm erkennbaren Gefässveränderungen auf die Schädigung der Funktion des umgebenden Lungenparenchyms in einem einzelnen Segment schliessen und entscheiden, ob eine Atelektase reversibel oder irreversibel ist, ob das unter einem Kollapsverfahren liegende Lungengewebe nach der Dekortikation seine Funktion in befriedigender Weise wieder aufnimmt oder nicht.

Besonders eindrucksvolle Bilder erhielten wir bei der angiographischen Untersuchung des Lungengewebes bei spezifischen und unspezifischen Empyemresthöhlen (Abb. 16).

3. Zu einem Abbruch einer Segment- oder Lappenarterie kommt es bei grösseren isolierten Lungenherden (Tuberkulom, Kavernen, grosse fibrokaseöse Nekrosen, Bronchialkarzinom, Lungenabszess) durch Zer-

Abb. 18. Postoperatives Angiogramm einer resezierten linken Lunge: vollständige Schrumpfung des Oberlappens, Kaverne in S^{1+2}, Emphysem des linken Unterlappens, normales Gefässsystem im antero-basalen Segment S^8, Rarefizierung und Einengung der Gefässe der übrigen Segmente als Zeichen der spezifischen Streuung.

störung des versorgenden Gefässes. Auch hier ist die Beurteilung des umgebenden Lungengewebes im Hinblick auf die von dem Hauptherd ausgehende Zerstörung ein wichtiger Faktor bei der funktionellen Beurteilung.

4. Das Emphysem, entweder in Form eines physiologischen Altersemphysems oder als strenger lokalisiertes, perifokales Emphysem in der Umgebung schrumpfender Prozesse, bedeutet ebenfalls eine funktionelle Schädigung des Lungengewebes. Durch den Schwund der Septen kommt

s zum Zusammenfliessen grösserer Acini, wodurch auch das Kapillarebiet der Alveolen teilweise zu Grunde geht. Angiographisch kann man iese Vorgänge deutlich verfolgen. Es kommt zum teilweisen Ausfall leinster Gefässverzweigungen, zur Auseinanderspreizung der noch estehenden Endverzweigungen und zur Kaliberabnahme grösserer rterien infolge der Streckung durch das vermehrte Lungenvolumen Abb. 17).

Das in einzelnen Segmenten durch schrumpfende Prozesse hervorgeufene, ganz verschieden starke und manchmal streng lokalisierte Emhysem lässt sich mit keiner Methode so differenziert nachweisen wie it der Angiographie. Bei der Gesamtbeurteilung des kardiorespiratorichen Systems im Hinblick auf eine geplante Lungenresektion spielen Ausmass und Stärke eines angiographisch sichtbaren Emphysems ine grosse Rolle, da es sich um funktionell minderwertiges Parenchym handelt.

5. Die Gefässinjektion unserer Operationspräparate mit Kontrastmittel und der Vergleich mit den vor der Resektion ausgeführten Angiogrammen und den histologischen Befunden zeigt, dass sich alle im präoperativen Angiogramm erkennbaren, für die verschiedenen Arten der Parenchymschädigung bezeichnenden Veränderungen auch im postoperativen Angiogramm reproduzieren lassen (Abb. 18). Wir schliessen daraus, dass weder funktionelle Vorgänge noch Einflüsse des hypertonischen Kontrastmittels bei der Erklärung der angiographischen Symptomatologie eine wesentliche Rolle spielen können. Die Veränderungen sind rein anatomisch bedingt, können jedoch für die funktionelle Beurteilung ausgewertet werden.

ZUSAMMENFASSUNG

Erfahrungen mit der selektiven Lungenangiographie mit Hilfe des Herzkatheters an 250 Kranken werden mitgeteilt. Anatomie und röntgenologische Kennzeichen der normalen Segmentarterien werden beschrieben. Die selektive Lungenangiographie bewährte sich besonders bei der funktionellen Beurteilung des einzelnen Lungensegmentes im Hinblick auf geplante Lungenteilresektionen. Deshalb werden die wichtigsten Kennzeichen pathologisch veränderter Segmentarterien im Röntgenbild, die durch Vergleich der histologischen Untersuchung der Operationspräparate mit den Angiogrammen gewonnen wurden, beschrieben.

SUMMARY

The authors report their experiences in a material of 250 cases of selective angiography of the lungs by means of heart catheters. The anatomy and roentgenologic appearances of the normal arteries of the segments are described. Selective angiography of the

lung is considered of particular value in the functional assessment of an individual segment in cases of proposed resection of a part of a lung. The more important roentgenologic signs of pathologically altered segmental arteries, which have been arrived at by a comparison of the information obtained from the histologic examination of the operation specimen and the angiogram, are presented.

RÉSUMÉ

Les auteurs présentent les constatations qu'ils ont faites sur une série de 250 cas d'angiographie sélective du poumon par cathétérisme du cœur. Ils décrivent l'anatomie et les aspects radiologiques des artères normales des segments. Ils considèrent que l'angiographie sélective du poumon est particulièrement utile pour juger la fonction d'un segment pulmonaire donné quand on se propose de faire une résection pulmonaire partielle. Les auteurs présentent les signes radiologiques les plus importants d'altération pathologique des artères segmentaires, qu'ils ont définis en comparant les données de l'examen histologique de la pièce opératoire avec l'angiographie.

SCHRIFTTUM

AMEUILLE, P., RONNEAUX, G., HINAULT, V. et LEMOINE, J. M.: Remarques sur quelques cas d'artériographie pulmonaire chez l'homme vivant. Bull. Soc. méd. Hôp. Paris 60 (1936), 729.

ANDERSEN, P. Th., ANDERSEN, I., ELTORM, H., POULSEN, Th., GLISTRUP, E. and PETERSEN, H.: Angiopulmography. Acta radiol. 36 (1951), 257.

BOLT, W., FORSSMANN, W. und RINK, H.: Selektive Lungenangiographie in der präoperativen Diagnostik und in der inneren Klinik. G. Thieme, Stuttgart 1957.

BOYDEN, E. A.: Segmental anatomy of the lungs. Blakiston Division. McGraw-Hill, New York 1955.

CARVALHO, L.: Angiocardiography. Dis. Chest. 17 (1950), 312.

CICERO, R. and DEL CASTILLO, H.: Lobar and segmental angiopneumography in pulmonary disease. Acta radiol. 45 (1956), 42.

COURNAND, A., BING, R. J., DEXTER, L., DOTTER, C., KATZ, L. N., WARREN, J. V. and WOOD, E.: Report of Committee of Cardiac Catheterization and Angio-cardiography of the American Heart Association. Circulation 7 (1953), 769.

DOTTER, CH. T. and STEINBERG, J.: Angiocardiography. Hoeber, New York 1951. (= Ann. Roentgenol. Vol. 20.)

FORSSMANN, W.: Geschichtliche Entwicklung und Methodik der Herzkatheterung. Ihr Anwendungsgebiet unter besonderer Berücksichtigung der Lungenerkrankungen. Arch. klin. Chir. 279 (1954), 450.

HANSEN, A. T.: Direkte Blutdruckmessung mittels eines Kondensatormanometers. Verh. dtsch. Ges. KreislForsch. 15 (1949), 97.

HANSON, H. E.: Temporary unilateral occlusion of pulmonary artery in man. Acta Chir. scand. Suppl. 187 (1954).

VON HAYEK, H.: Die menschliche Lunge. Springer, Berlin 1953.

HORNYKIEWYTSCH, TH. und STENDER, HH.: Normale und pathologisch veränderte Lungengefässe im Schichtbild. Fortsch. Röntgenstr. 79 (1953), 44, 639, 704; 80 (1954), 458; 81 (1954), 36, 134, 455, 642; 82 (1955), 228, 331, 642.

JANKER, R.: Röntgenologische Funktionsdiagnostik mittels Serienaufnahmen und Kinematographie. W. Giradet, Wuppertal-Elberfeld 1954.

JÖNSSON, G., BRODÉN, B. and KARNELL, J.: Selective angiocardiography. Acta radiol. 32 (1949), 486.

LÖFFLER, L.: Die Arteriographie der Lunge und die Kontrastdarstellung der Herzhöhlen am lebenden Menschen. Georg Thieme, Leipzig 1955.

LÖHR, HH., SCHOLTZE, H., KLINNER, W. und ZENKER, R.: Zur Indikationsstellung bei der chirurgischen Behandlung der spezifischen und unspezifischen Empyemresthöhle auf Grund der selektiven Lungenangiographie. Arch. klin. Chir. 283 (1957), 1.

NEUHAUS, G.: Eine Methode zur fortlaufenden, blutigen Registrierung intrakardialer und vaskulärer Drucke. Verh. dtsch. Ges. KreislForsch. 16 (1952), 201.

NORDENSTRÖM, B.: Temporary unilateral occlusion of the pulmonary artery. Acta radiol. (1954) Suppl. No. 108.

RIMINI, R. y RODRIGUEZ, A.: La angioneumografia en la tuberculosis pleuropulmonar. An. Fac. Med. Montevideo 1952.

ROBB, G. P. and STEINBERG, J.: Visualization of the chambers of heart, pulmonary circulation and great blood vessels in man: Practical method. Amer. J. Roentgenol. 41 (1939), 17.

SCHOENMACKERS, J. und VIETEN, H.: Atlas postmortaler Angiogramme. Georg Thieme, Stuttgart 1954.

SCHOLTZE, H., KLINNER, W. und LÖHR, HH.: Sind die im Angiogramm bei der chronischen Lungentuberkulose erkennbaren Veränderungen funktioneller oder anatomischer Art? Beitr. Klin. Tuberk. 117 (1957), 244.

STUTZ, E. und VIETEN, H.: Die Bronchographie. Georg Thieme, Stuttgart 1955.

VIETEN, H.: Persönliche Mitteilung.

ZENKER, R., HEBERER, G. und LÖHR, HH.: Die Lungenresektionen. Anatomie, Indikationen, Technik. Springer, Heidelberg 1954.

FROM THE GUSTAF WERNER INSTITUTE FOR NUCLEAR CHEMISTRY AND THE INSTITUTE OF ANATOMY, UNIVERSITY OF UPPSALA, SWEDEN

EFFECT OF HIGH ENERGY PROTONS ON THE SPINAL CORD

by

Börje Larsson, Lars Leksell, Bror Rexed,
and *Patrick Sourander*

During the last decade experiments have been performed to produce localized lesions in the central nervous system with various kinds of ionizing radiations. CAMPBELL and NOVICK (1949) implanted 'radon seeds' in the cerebral cortex of the cat, and GLOBUS et coll. (1952) in the medulla oblongata of the dog. Radioactive isotopes were placed intracranially by *e. g.* AJURIAGUERRA et coll. (1954) with Au^{198}, and BOGUMILL (1957) with Co^{60}. ARNOLD et coll. (1954) investigated the effect of a 1 cm broad 23 MeV roentgen beam from a betatron on the brain of the monkey. ANDERSON et coll. (1957) irradiated the hypothalamus in the rat with 190 MeV deuterons, using the technique devised to irradiate the hypophysis by TOBIAS et coll. (1954). An interesting use of relatively low energy protons, 10 MeV, was reported recently by MALIS et coll. (1957) who employed the thin ionization peak at the end of the proton beam to produce narrow lesions at a depth of 0.8 mm in the cerebral cortex of the cat.

If the aim is to irradiate selectively small restricted regions situated deeply in the brain, narrow beams of high energy heavy particles show

Submitted for publication 28 May 1958.

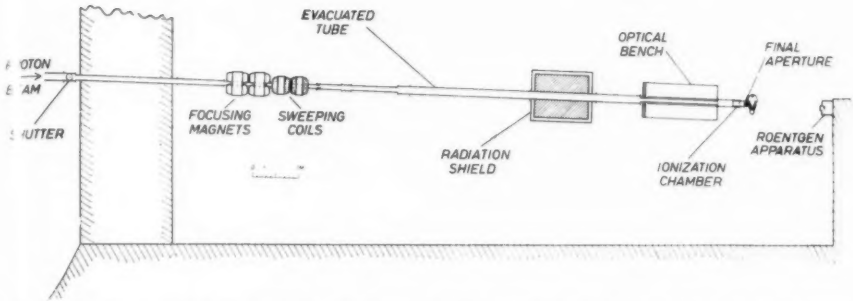

Fig. 1. Plan for irradiation of rabbit's spinal cord with high energy protons from the synchrocyclotron. The 'optical bench' permits accurate alignment of the instruments used for measuring the dose and for collimating the beam. The animals were positioned by means of a roentgen apparatus. The doses were checked and the beam controlled from a shielded control area.

great advantage because of their very low scattering. By a stereotaxic method and rotation of the object or cross fire technique the radiation dose can be concentrated on any desired site. Such a technique has been described by LEKSELL (1951), who used roentgen beams for focal irradiation of deep cerebral structures.

The development of modern particle accelerators means that more effective appliances for producing high energy particle beams will be available for radiosurgical use. In this case as in other radiobiological experiments one would have to consider the prolonged effects, the nature of which will take a long time to appear. It is therefore of great importance that investigations should be started as soon as possible to determine the effect of such ionizing beams on different parts of the central nervous system. The present investigation is the first part of such a study conducted with the 185 MeV proton beam from the 230 cm synchrocyclotron in Uppsala. This beam has a range of 21 cm in tissue and shows very low scattering in the first half of its course.

Material and methods

Radiation technique. The irradiations were performed with a 185 MeV proton beam from the 230 cm synchrocyclotron at the Gustaf Werner Institute. The beam has been applied for local irradiation under reproducible conditions. It is extracted by a regenerative deflector as suggested by LE COUTEUR and focused by two pairs of quadrupole magnets. The first pair, close to the cyclotron, collimates the diverging proton bundle to an almost parallel beam which is brought to a shielded exposure room (Fig. 1). The second pair of magnets, 10 m in front of the object, improves parallelism and determines the cross sectional structure of the beam. Two sweeping coils sweep the beam vertically and horizontally at a point immediately beyond the second magnet pair. In this way the strong-

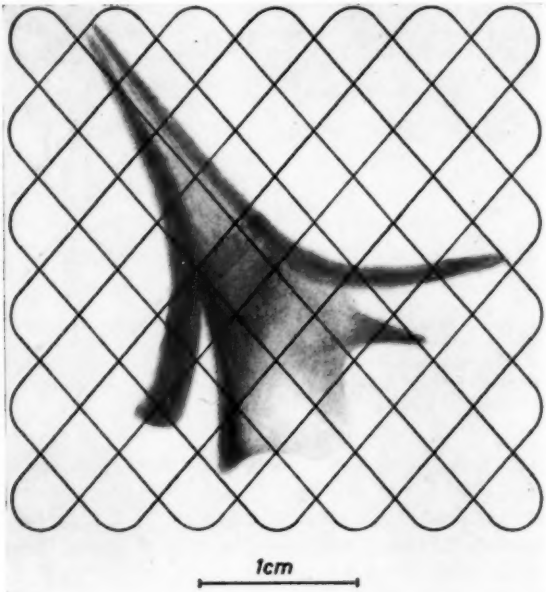

Fig. 2. Sketch showing how the beam cross section was homogenized. Shaded area: Auto-radiogram of the beam immediately before entering the ionization chamber. The sweeping coils fed with sawtooth current moved the beam along the indicated lines forming a Lissajou pattern. This procedure repeated with a frequency of 6 c/min made it possible to apply a uniform radiation field with minimal loss of protons.

ly nonhomogeneous beam cross section is smoothed out, and objects of different sizes can be irradiated with a minimal loss of protons. From the point of view of the object the protons seem to emerge from a 1×2 cm 'focus' at a distance of 8 m. The beam proceeds through an evacuated tube so that no scattering is introduced before the protons leave it through a thin mylar window (10 mg cm^{-2}) immediately in front of the ionization chamber, which measures the density of the proton flux. The desired beam profile is brought about by a final aperture.

In this experiment two ionization chambers of different types were used. The first one was a plane parallel 'transverse' chamber with the collection field parallel to the direction of the beam and introducing 600 mg cm^{-2} of scattering material. After a time a 'longitudinal' chamber with the collecting field perpendicular to the direction of the beam was substituted for this chamber. In this way the amount of scattering material was decreased to 25 mg cm^{-2} including the gas, nitrogen, at atmospheric pressure. The final beam aperture was 40 cm beyond the transverse chamber and immediately beyond the longitudinal chamber. The distance between the final aperture and the spinal cord was in both cases 10 cm. A detailed description of the apparatus and the measuring technique will be given in a technical report.

The mean dose rate (*i. e.* during ca 10 sec) was 1,000 to 2,000 rad/min. During

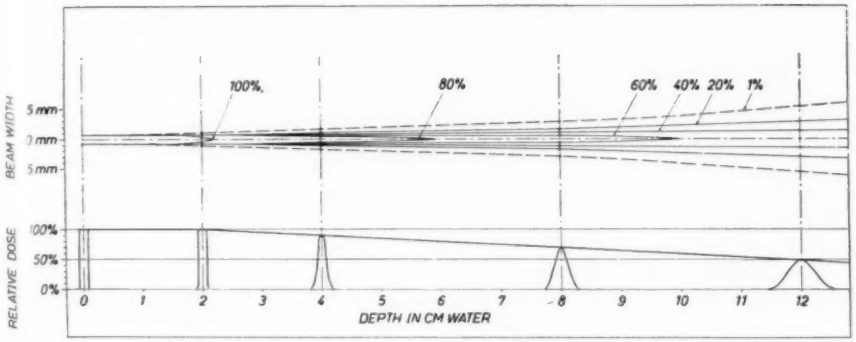

Fig. 3. Isodose curves from the 1.5 mm beam plotted from photographic measurements in a water phantom. The lower part of the figure shows relative doses at different depths. The beam does not widen appreciably in its early course in the region corresponding to the position of the spinal cord at a depth of 3.5 cm. The doses refer to the entrance dose.

each irradiation the normal variations were within $\pm$ 10 % of the mean value. The dose appears in pulses of ca 10 microseconds duration 240 times per second. This dose-time function is further modulated by the homogenizing sweeping of the beam. It is defined by the sweep frequencies and amplitudes, and by the structure and size of the beam cross section. Symmetrical sawtooth sweeping was used both horizontally and vertically. The frequencies, 0.6 and 0.7 c/sec respectively, gave a Lissajou figure of the order 6 : 7 (Fig. 2). The double sweep amplitude was 3.5 cm in both directions. The uniformity of the flux density in the beam cross section was checked by analysing the induced C^{11}-activity in a mosaic of small pieces of polythene, irradiated in a plane perpendicular to the beam and immediately in front of the final aperture.

Two different slit-shaped apertures were used, 1.5 and 10 mm wide. The dose distributions were calculated from density measurements on photographic films exposed in a water phantom at the position of the spinal cord and calibrated in terms of relative dose (Fig. 3).

Biological methods. 26 rabbits weighing 2 to 3 kg were used. The proton beam was directed to the lower thoracic region of the spinal cord. The spinal cord provides a suitable region to evaluate the effect of radiation on nervous tissue because of its regular arrangement of grey and white matter; in addition the disturbance of function is easy to observe. The animals were irradiated with 185 MeV protons under deep intravenous nembutal anaesthesia. During the experiment the animal was suspended from the experimental stand by steel supports inserted into the musculature of the back. A roentgenogram superposed on the autoradiogram of the thin proton beam showed the position of the beam in relation to the spinal column (Fig. 4). In most instances a roentgen examination was made after the irradiation and showed that movements of the spinal column at right angle to the beam seldom occurred. The possibility of small movements having occurred cannot, however, be excluded. During the irradiation the animals were watched by means of mirrors, and if any obvious movement was seen the experiment was discontinued.

After irradiation the animals were observed regularly, motor function and sensation being tested, and neurological symptoms noted. In most cases paresis of varying degree developed. The animals were killed by exsanguination under chloroform anaesthesia at

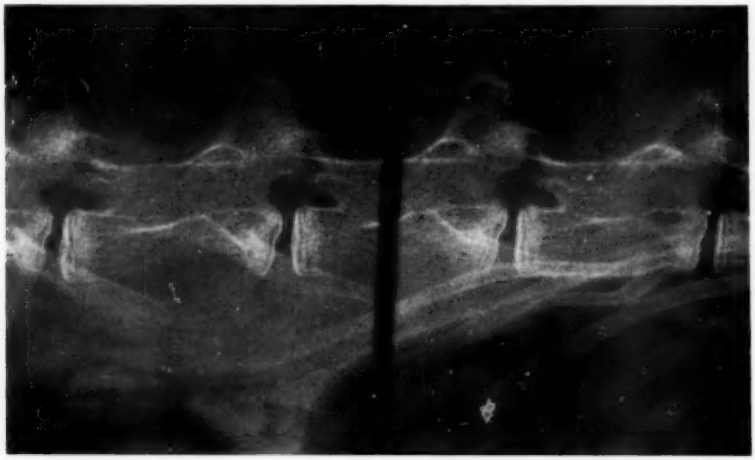

Fig. 4. Autoradiogram of the proton beam — the black vertical band — superposed on a roentgenogram of the rabbit's spinal column. × 1.5.

different periods following the appearance of the paresis. In this report the longest survival period after irradiation was 9 months. Animals, which had received a low dose of radiation, survived longest. Of these animals 3 are still living without obvious changes.

Histological technique. The spinal cords were removed within their dural sac and most of them were fixed in 5 % neutral formol-saline for 2 to 4 weeks. A few spinal cords were fixed in formol-ammonium bromide so that the glial cells could be studied. The irradiated part of the spinal cord was in most cases visible to the naked eye. This part of the cord and a considerable portion of the tissue on either side of it, was taken for histological examination. Frozen sections, 15 μ thick, were made, or the cord was embedded in paraffin and cut at 10 μ. The cord was cut longitudinally and in serial sections in a frontal plane. This made it possible to examine in the same section the irradiated zone and a considerable part of the surrounding tissue. In a few cases cross sections of the cord were made.

Twenty-three spinal cords were studied. The following staining methods were used: Heidenhain's myelin sheath stain, Palmgren's silver impregnation of axons, toluidin blue stain for the Nissl substance of the nerve cells, Ranke's, Holzer's, Cajal's and Rio del Hortega's methods for glial cells, Azan and hematoxylin van Gieson for connective tissue and blood vessels, Turnbull's blue to study the presence of iron, and Scharlach red for fat.

Experimental results

Effect of single radiation dose of 20,000 rad using a narrow beam

Preliminary experiments showed that a single dose of 20,000 rad produced well defined damage of the spinal cord after a relatively short latent period. In 8 animals this dose was given with a beam 1.5 mm broad.

Fig. 5. Longitudinal section of rabbit's spinal cord; myelin preparation showing localized damage 12 days after irradiation with a 1.5 mm beam of high energy protons. Dose: 20,000 rad. Heidenhain stain. × 9.

No change was observed in any of the animals for 1 week. The first neurological symptoms appeared usually 8 days after irradiation and consisted of lively tendon reflexes in the hind legs and slight knee and ankle clonus. In 3 of the animals flaccid paresis of the lower trunk musculature and hind legs together with weak or practically abolished tendon reflexes occurred on the 9th day, and in 2 others considerably later, *i. e.* 3 and 5 weeks respectively after radiation. Of these animals, 1 was killed immediately after the appearance of paresis and the others 3 to 7 days later. No paresis appeared in 3 animals within 6 months, probably because the animals did not receive the effective dose on account of their movement during irradiation. The animals had, however, lively tendon reflexes and slight clonus in the hind legs.

Macroscopy. Epilation or other changes were not found in any of the animals on the outer aspect of the skin. The inner surface of the skin and the muscle presented a sharply delimited lesion 1.5 to 2 mm broad corresponding to the path of the beam. The lesion in the muscle was more evident at the side of entering than at the side of exit. The lesion in the skin and muscles was characterized by hyperaemia and necrosis of varying degree. In the meninges and the cord, a band 2 mm wide of grayish discolouration marked the radiated portion of the cord. No haemorrhages or inflammatory signs were seen in the spinal canal and the meninges.

Microscopy. The histologic changes in the spinal cord of 5 animals, killed $^1/_2$ to 7 days after the appearance of the paresis, were almost identical. A narrow and sharply delimited zone was destroyed; this corresponded to the path of the beam. The lesion was slightly broader in the white substance and had about the same breadth as the proton beam (Fig. 5). The damaged grey substance was only about half the breadth of the beam. These measurements apply only to the fixed material since corrections for shrinkage were not made. In longitudinal sections of the cord the lesion had a 'butterfly' contour. The lesion in both white and grey substance was that of acute necrosis affecting nerve cells, axons, myelin

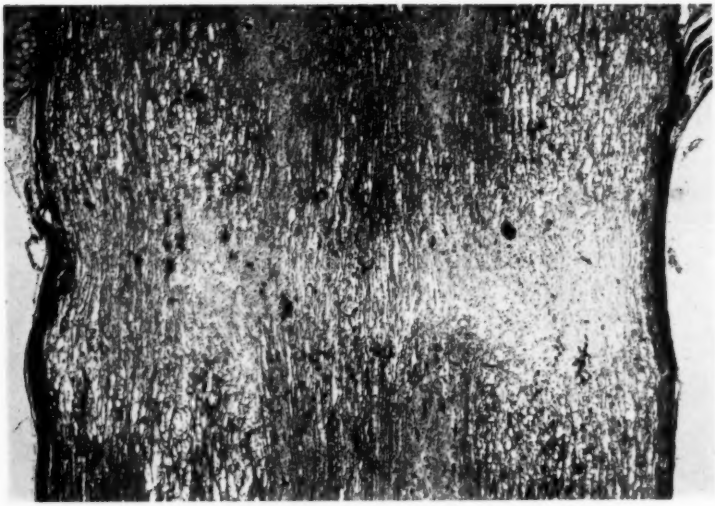

Fig. 6. Longitudinal section of rabbit's spinal cord 11 days after irradiation with a 1.5 mm beam of high energy protons. Small perivascular haemorrhages are seen in the track of the beam as black rounded masses. Dose 24,000 rad. Azan stain. × 25.

sheaths and glial cells. Evidence of a selective radiation effect on the various components of the neural tissue was not seen. Minimal haemorrhages surrounding capillaries and small veins were found at the borderline of the lesion, and they were also seen in a few cases in the middle of the irradiated zone (Fig. 6). Sometimes a large aggregation of erythrocytes and hyaline thrombus were evident in dilated small vessels within the disintegrating tissue. Massive haemorrhages were not seen in any of the cords. Chromatolysis of nerve cells and occasional nerve cells undergoing neuronophagia and slight gliomesenchymal cell proliferation occurred in a small marginal zone between the irradiated and nonirradiated tissue (Fig. 7). In the white substance this zone was characterized by degeneration of myelin sheaths and axons. In all the animals a small number of intact nerve fibres were present in the subpial parts of the spinal cord. In animals killed 7 days after the paresis appeared, a number of gitter cells were evident at the edge of the necrosis as well as occasional glial cells containing iron pigment. Fat staining was always negative.

Secondary Wallerian degeneration of the transected spinal cord tracts had developed in a few cases.

In animals which did not present any paresis, the histologic changes of the spinal cord were very slight or wholly lacking.

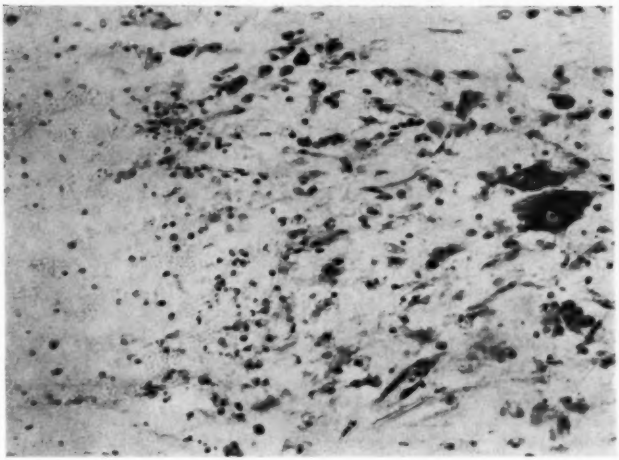

Fig. 7. Longitudinal section of rabbit's spinal cord showing the sharp demarcation of the irradiated zone to the left. Bordering the irradiated zone is a band of nuclear fragments, and adjacent to them numerous glial cells; further away nerve cells are present. Proton beam 1.5 mm broad. Dose 20,000 rad. Thionin stain. × 150.

Effect of a single radiation dose greater or smaller than 20,000 rad using a narrow beam

The approximate relationship between dose and time of appearance of signs was studied in 11 animals irradiated with the following doses: 40,000, 24,000, 16,000, 12,000, 10,000, 8,000 and 5,000 rad.

After a dose of 40,000 rad progressive paralysis of the hind legs and axial musculature along with paresis of the bladder appeared within 2 days. The animal was killed 5 days after irradiation and then showed necrosis of the spinal cord considerably more extensive than that seen after a dose of 20,000 rad. Small but rather numerous haemorrhages appeared at the edge of the necrosis and also in the irradiated nerve roots and spinal ganglia. In addition a small necrotic zone, probably the result of vascular damage, was present on either side of the track of the beam.

A dose of 24,000 rad produced the same effects as 20,000 rad (Fig. 6).

With doses less than 20,000 rad the period between irradiation and the appearance of signs was longer. In 3 animals irradiated with 16,000 rad the appearance of the lesion was studied at a relatively late stage, 2 and 3 weeks respectively after the onset of paresis. In all the cases typical radiation necrosis was seen. There was active resorption of the

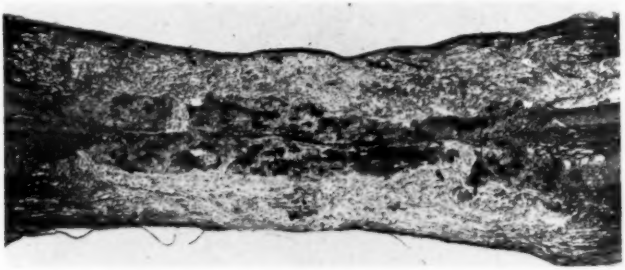

Fig. 8. Longitudinal section of rabbit's spinal cord; myelin preparation showing extensive necrosis and multiple perivascular haemorrhages 4 days after irradiation with a 10 mm high-energy proton beam. Dose 20,000 rad. Heidenhain stain. × 8.

necrotic material and a large number of gitter cells in the sharply demarcated cystic cavities in the white substance. The structure of the tissue could partly be recognized in the grey matter which was less damaged than the white. Slight proliferation of protoplasmic and fibrillary astrocytes and also a few very small haemorrhages occurred around the necrosis. The demarcation zone was even in these cases sharply defined. Secondary Wallerian degeneration had taken place in the adjacent parts of the spinal cord. Animals irradiated with 12,000 rad or less did not, over a year or more, show any clinical signs or histologic changes in the spinal cord.

Effect of a single radiation dose of 20,000 rad using a broad beam

To study the relationship between the breadth of the beam and the type of radiation damage, a group of 7 animals were irradiated in the same manner as the first series but with a beam 10 mm broad instead of 1.5 mm.

The animals showed brisk reflexes in the hind legs 2 days after radiation. After 3 to 4 days paresis of the musculature appeared and quickly progressed to paralysis of the whole hind part of the body with bladder paresis and loss of pain sensation. These animals were killed 1, 2, 3, 4, 5, and 6 days after irradiation to study the development of the radiation necrosis.

Macroscopy. The inner side of the skin did not show any changes during the first few days, but later a hyperemic region a little broader than 10 mm appeared. As early as 1 day a fairly sharply delimited hyperaemic haemorrhagic zone was seen in the muscles and was of the same breadth or a little broader than the beam. After 1 to 3 days the meninges

nd spinal cord presented hyperemia of the irradiated region, and after to 6 days numerous petechial bleedings.

Microscopy. After 1 and 2 days the grey substance of the cord showed nany dilated capillaries and veins containing large aggregations of rythrocytes. The nerve cells, axons, myelin sheaths and glial cells ppeared to be intact.

After 3 days the grey matter within a zone about 10 mm wide showed narked exudation of plasma as well as multiple and somtimes rather rge haemorrhages (Fig. 8). The nerve cells were undergoing chromato- ysis and cytolysis. The white matter was relatively spared and showed nly perivascular oedema and less marked staining of the myelin in the erivascular zone. Throughout the track of the beam in the meninges nd cord a slight inflammatory cellular proliferation was seen around the vessels. After 4 to 6 days the changes in the grey substance were nore accentuated and the white substance showed widespread degenera- tion and necrosis; adjacent to the track of the beam some degenerate areas, probably of vascular origin, were evident.

Discussion

The experiments described show that it is possible to cause sharply delimited acute lesions of the central nervous system with a narrow beam of high energy protons. The lesion in the white matter of the spinal cord has approximately the same dimension as the breadth of the proton beam used. In the grey substance changes arise in a zone somewhat thinner than the beam. The lesion is that of an acute necrosis and similar to that described by ARNOLD and co-workers after irradiation of the brain in the monkey with high energy roentgen radiation.

It is a common characteristic of damage caused by different kinds of ionizing radiation that a certain latent period occurs between the irradiation of the tissue and the appearance of functional and morphological effects. In our experiments as well as those of ARNOLD and co-workers it appeared that the latent period for radiation necrosis of the central nervous system depends on the dose of radiation. A dose of 20,000 to 24,000 rad with a 1.5 mm broad proton beam gave a well defined lesion after 9 days. With larger and smaller doses the latent period was shortened or prolonged respectively.

The breadth of the beam proved to be a factor of great importance. In our experiments a 10 mm beam not only produced necrosis of about the same breadth as the beam but also produced a lesion considerably quicker than a thinner 1.5 mm beam. The broad lesion differed also

histologically in certain respects from that produced by the thinner beam. With the thin beam only slight vascular damage and minimal haemorrhages were seen; with the same dose and a broad beam even after one day signs of vascular damage and after 3 days marked plasma exudation and numerous haemorrhages appeared. The haemorrhages were localized especially to the grey substance; at this time only small focal destruction was evident in the white substance. The radiation necrosis proper was observed only after one day more. The severe vascular changes present after irradiation with the broad beam probably depended on the fact that a greater portion of the vascular bed of the spinal cord had been irradiated. The peculiar type of vascular arrangement in the spinal cord and the poor development of collaterals in its thoracic part probably favoured the appearance of large haemorrhages.

The fact that the vascular changes appeared at the time when only slight destruction of the myelin sheaths could be seen is of great interest. This circumstance stresses the fact that vascular changes may be among the causal factors of delayed radiation necrosis in the nervous system. According to ARNOLD and co-workers the necrosis appears quite independently of the effects on the circulatory system and as a direct effect of the radiation. In all the irradiated spinal cords in our material, whatever the radiation dose or the breadth of the beam, a thin peripheral zone of the spinal cord with intact axons and myelin sheaths persisted in the irradiated region. This observation also stresses the importance of vascular factors, since it is well known that the peripheral region of the spinal cord is more resistant to a damaged circulation than the more central parts of the cord.

The present investigations concern only the acute lesions. The type and extent of similarly produced lesions in a late stage are being studied in the brain and will be the subject of a future publication. The present experiments show that with the help of a high energy proton beam it is possible to cause a small and sharply restricted zone of acute necrosis in the central nervous system. This is of considerable interest in experimental investigations for studying the effects of lesions in various parts of the nervous system.

Acknowledgements

The authors wish to thank Prof. The Svedberg for his great interest in this work and for extending the facilities of his laboratory, Prof. C. A. Tobias for generously sharing his experience of the radiological use of the Berkeley 184 inch cyclotron, Å. Svanheden and K. W. Ståhl for valuable technical cooperation, the cyclotron crew for their help and protons, and Miss M. Johansson for making the preparations. The investigation has been supported by the Swedish Medical Research Council and the Office of Scientific Research of the Air Research and Development Command, United States Air Force.

through its European Office, under Contract No. AF 61 (514)—1249. Part of the technical work was supported by the Swedish Technical Research Council and the Knut and Alice Wallenberg Foundation.

SUMMARY

The spinal cord in the rabbit has been irradiated with a 185 MeV proton beam from a 230 cm synchrocyclotron. Using a 1.5 mm broad beam it has been possible to effect sharply delimited lesions of the spinal cord with only minimal haemorrhages and without any general reactions. With a 10 mm beam the tissue reactions are much more severe. The histopathology of the acute radiation necrosis is described and the factors responsible for its appearance are discussed, especially the width of the proton beam and the size of the single radiation dose.

ZUSAMMENFASSUNG

Das Rückenmark des Kaninchens ist mit einem 185 MeV-Protonenstrahl eines 230 cm Synchrocyclotronen bestrahlt worden. Bei Anwendung eines 1.5 mm breiten Strahlenbündels ist es möglich gewesen, scharf begrenzte Veränderungen des Rückenmarkes mit nur minimalen Blutungen und ohne Allgemeinreaktionen zu erzeugen. Mit einem 10 mm breiten Strahl waren die Gewebsreaktionen viel ernster. Die Histopathologie der akuten Radionekrose wird beschrieben und die Faktoren, welche für das Auftreten dieser Nekrose verantwortlich sind, werden besprochen, besonders die Breite des Protonstrahlenbündels und die Grösse der Röntgendosis bei einmaliger Bestrahlung.

RÉSUMÉ

La moelle épinière de lapins a été irradiée par le faisceau de protons de 185 MeV émis par un synchrocyclotron de 230 cm. Avec un faisceau large de 1.5 mm il a été possible de créer des lésions nettement délimitées de la moelle, avec seulement des hémorragies minimes et sans aucune réaction générale. Les réactions tissulaires ont été beaucoup plus graves avec un faisceau de 10 mm. Les auteurs décrivent l'histopathologie de la radionécrose aiguë. Ils examinent les facteurs responsables de son apparition, en particulier la largeur du faisceau de protons et la dose de radiation administrée en une fois.

REFERENCES

De Ajuriaguerra, J., Benda, Ph., Constans, J., David, M. et Tubiana, M.: Étude expérimentale des lésions provoquées par l'implantation intracérébrale de fragments d'or radioactif. Rev. Neurol. (Paris) 91 (1954), 260.

Anderson, A., Garcia, J., Henry, J., Riggs, C., Roberts, J. E., Thorell, B. and Tobias, C. A.: Pituitary and hypothalamic lesions produced by high-energy deuterons and protons. Rad. Res. 7 (1957), 299.

Arnold, A., Bailey, P. and Laughlin, J. S.: Effects of betatron radiations on the brain of primates. Neurology 4 (1954), 165.

Bo[illegible]umill, G. P.: Tissue changes in the brains of cats and monkeys following cobalt 60 irradiation. Neurology 7 (1957), 245.

CAMPBELL, B. and NOVICK, R.: Effects of beta rays on central nervous tissues. Proc. Soc. exp. Biol. 72 (1949), 34.

GLOBUS, J. H., WANG, S. C. and MAIBACH, H. J.: Radon implantation in the medulla oblongata of the dog; effects on the degree and extent of cellular reactions. J. Neuropath. 11 (1952), 429.

LE COUTEUR, K. J. and LIPTON, S.: Non-linear regenerative extraction of synchrocyclotron beams. Phil. Mag. 46 (1955), 1265.

LEKSELL, L.: The stereotaxic method and radiosurgery of the brain. Acta chir. scand. 102 (1951), 316.

MALIS, L. I., LOEVINGER, R., KRUGER, L. and ROSE, J. F.: Production of laminar lesions in the cerebral cortex by heavy ionizing particles. Science 126 (1957), 302.

TOBIAS, C. A., VAN DYKE, D. C., SIMPSON, M. E., ANGER, H. O., HUFF, R. L. and KONEFF A. A.: Irradiation of the pituitary of the rat with high energy deuterons. Amer. J Roentgenol. 72 (1954), 1.

FROM NORSK HYDRO'S INSTITUTE FOR CANCER RESEARCH, THE NORWEGIAN RADIUM HOSPITAL, OSLO, NORWAY

DEPTH DOSE DISTRIBUTION USING POINT SOURCES OF Cs^{137} FOR PLESIOTHERAPY

by

Johan Baarli

Therapy units, usually containing several grams of radium, have been widely employed for the radiotherapy of metastases, particularly in the glands in the supraclavicular region. Due to the relatively low radiation output from the radium units, it has been necessary to employ a short SSD (source skin distance) which means that a steep drop occurs in the dose with depth. The advantage of using this kind of treatment is that tumours located down to a few centimeters below the skin can be treated by radiation in such a way that heavy doses to the underlying healthy tissue can be avoided. The greater energy of the radiation from radium also induces a less severe erythema reaction compared to the use of highly filtered roentgen rays for the same purpose. Radiation treatment of this kind is referred to as plesiotherapy where a short SSD is used.

The low radiation output, and consequently the inconveniently protracted treatment times, with these radium units, have resulted in the conversion of many of the teleradium units to similar cobalt units where the radium packs have been replaced by artificially produced Co^{60}. Especially constructed units of the same kind using Co^{60} and Ir^{192} have also been reported (LINDELL & WALSTAM 1956, MITCHELL 1951).

Submitted for publication 21 March 1958.

The radioactive isotope Cs^{137} has recently been made available in larger quantities (AEBERSOLD 1955, COCKROFT 1957) and this isotope has been suggested as a very important radiation source for future radiotherapy (BRUCER). Considerations of its physical and radiation properties seem to indicate that this isotope may be well suited for plesiotherapeutic application (BAARLI 1958).

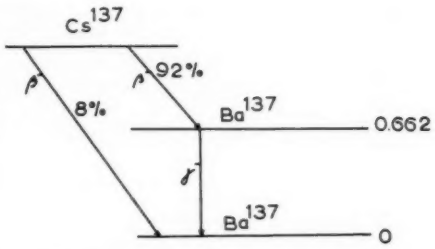

Diagram 1. The decay properties of Cs^{137}.

The radiation properties from Cs^{137} are shown in Diagram 1. It decays with a half-life of 28 years emitting two β-particles with energies of 1.2 and 0.51 MeV. The emission of the 0.51 MeV β-particles result in an excited state of Ba^{137} which decays to the stable nuclei by emission of one single γ-ray line with an energy of 662 keV. The decay of Cs^{137} occurs with 92 % via the excited state and 8 % decays directly to the stable state of the Ba^{137} nuclei.

It is because of the mono-energetic γ-ray of 662 keV and its long half-life, 28 years, that Cs^{137} has attracted great interest for therapeutic application.

Cs^{137} is produced by fission of U^{235} with a high degree of probability and is accumulated as a waste-product in the uranium fuel rods used for production of atomic energy in the reactors. Due to the rapid development of such nuclear reactors it is to be expected that large quantities of this material will become available at a relatively low price in the future.

The radioactive material Cs^{137} is to-day commercially available in two chemical forms, CsCl and Cs_2SO_4, the specific activity being approximately 100 curies/cc.

The dose rate at one meter per curie of this material is calculated to 0.314 r per hour neglecting self-absorption (BAARLI & BRUSTAD). It is evident from this relatively low specific activity that greater quantities of this radioactive material are needed for therapeutic units. Some experimental and theoretical studies are now reported. These were carried out in order to determine the requirements for using a point source of this material in a plesiotherapy unit to operate at a focus-skin-distance between 5 and 10 cm.

Theoretical calculations

The depth-dose distributions or dose distribution along the central axis of the radiation field penetrating soft tissue is of the greatest interest to therapists. Due to the relatively complicated manner in which the radiation is absorbed when penetrating matter,

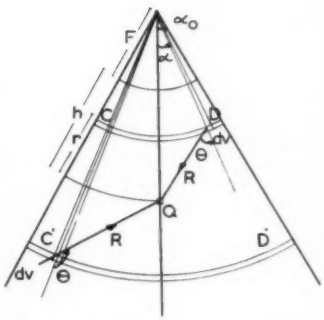

Diagram 2. The cross-section of the radiation field furnished with the parameters used for calculation of the dose distribution along the central axis when irradiated with 662 keV photons from Cs^{137}.

the most common way to establish depth-dose curves is by direct dose measurements. In spite of the complexity of the absorption processes, attempts have been made to calculate the distribution (LAMERTON and PAYNE-SCOTT) and good agreement with experiments has also been obtained under certain simplified conditions.

The present calculations have been carried out for a highly divergent circular beam of monoenergetic photons of 0.662 MeV from a point source of Cs^{137} entering an absorber of water. Except for the geometrical approximations the LAMERTON-procedure has been followed quite closely. This is based upon calculating the primary radiation intensity decrease with depth and adding to this the intensity contribution from the singly and multiply scattered radiation.

The intensity distribution has then been converted to dose.

Diagram 2 shows a cross-section of the radiation field furnished with the parameters used for the calculations, α_o being the maximum angle of the field, F the SSD. Q is the point on the central axis where the intensity is calculated, and h the distance from the surface to point Q. Due to ease in the integration procedure the irradiated surface was given a spherical shape with radius F.

If P_o is the intensity of the primary radiation at the surface, then the intensity of the primary radiation at Q is given by the following expression in which μ_o is the linear absorption coefficient for the primary radiation

$$P_h = P_o \frac{F^2}{(F+h)^2} e^{-\mu_o h} \tag{1}$$

The singly scattered radiation reaching Q has to be integrated over the whole irradiated volume. This radiation is proportional to the intensity of the primary beam at D which may be expressed by:

$$P_{h-r} = P_o \frac{F^2}{(F+h-r)^2} e^{-\mu_o (h-r)} \tag{2}$$

Assuming now that the volume element dv has the form of a ring at the depth $(h-r)$, each electron in this will scatter the primary photons according to the KLEIN-NISHINA formula. This function is given by $f(\cos \Theta)$ and expresses the intensity of the scattered photons in the direction Θ per electron per unit solid angle. Now, if η is the number of electrons per cm^3 and R the distance from D to Q, then the intensity of the once scattered radiation, from the volume dv reaching Q per unit solid angle is given by:

$$dI_s = \frac{1}{R^2} e^{-\mu_o (\Theta) R} P_{h-r} f(\cos \Theta) \eta \, dv \tag{3}$$

where $\mu_o(\Theta)$ is the total linear absorption coefficient of the singly scattered radiation from dv, scattered at an angle Θ. This coefficient depends upon the angle of scattering. The total contribution of the radiation intensity caused by singly scattered radiation at Q

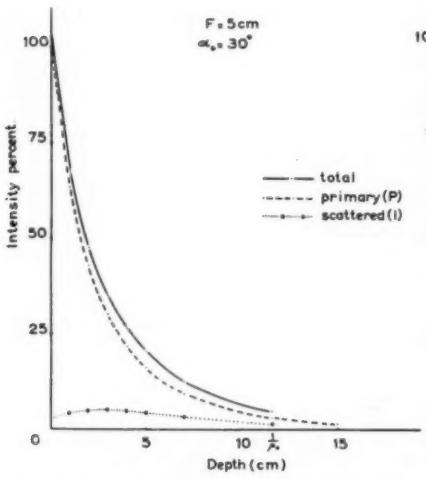

Diagram 3. Calculated depth-dose distribution for Cs^{137} (662 keV) and SSD 5 cm.

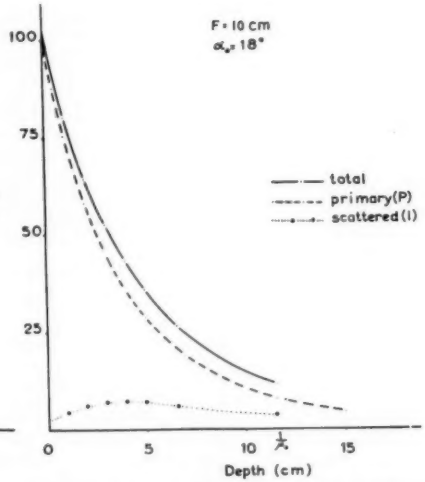

Diagram 4. Calculated depth-dose distribution for Cs^{137} (662 keV) and SSD 10 cm.

can now be calculated by integrating eq. (3) over the whole irradiated volume. This procedure has to be carried out numerically by choosing suitable free variables. For this purpose eq. (3) may be written:

$$I_s = Kff\,\psi\,(r, t)\,dr\,dt \tag{4}$$

where:

$$K = 2\pi\eta P_o F^2\, e^{-\mu_o h}, \quad t = 1 - cos\ a$$

and a is the angle indicated in Diagram 2, and

$$\psi(r, t) = \frac{1}{R^2}\, e^{-\mu_o r - \mu_o(\theta) R}\, f(cos\Theta)$$

where $f(cos\ \Theta)$ is the Klein-Nishina function.

The integration has to be carried out between the limits [0,1-cos a_o] for t, and [$-r_o$, h] for r.

The contribution of the intensity from the multiply scattered radiation has to be evaluated in an approximate way. It has to be noted that not only the volume determined by the primary radiation contributed to the multiply scattered radiation at point Q, but radiation scattered from the volume outside this can also contribute.

The singly scattered radiation is partially absorbed and partially scattered on its way from dv to Q. The scattering introduces the factor $e^{-\mu_s(\Theta)R}$ and the contribution to the intensity at Q is reduced in this way. On the other hand, Q will receive some contribution of radiation scattered more than once. Considering the total energy of the multiply scattered radiation, it can be assumed that this is somewhat less than the energy lost by scattering. It is therefore reasonable to assume that the contribution from the

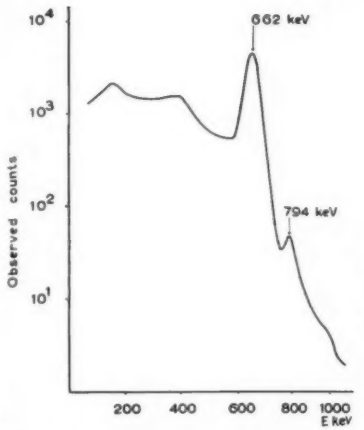

Diagram 5. Measured pulse-height distribution from the 5 curie Cs^{137} source.

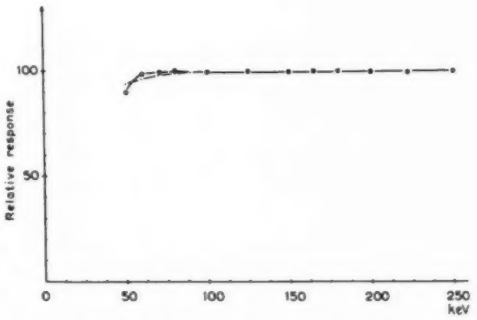

Diagram 6. The energy response of the scintillation dosemeter (unfilled circles) and ionization chamber (filled circles) relative to a 100 r Victoreen type thimble chamber.

multiply scattered radiation at Q can be compensated for by adding the singly scattered radiation lost by scattering. This can be done mathematically by substituting the total absorption coefficient for the singly scattered radiation $\mu_o(\Theta)$ with the real absorption coefficient $\mu_a(\Theta)$.

The contribution of the radiation intensity at Q caused by the total scattered radiation is then obtained by replacing $\mu_o(\Theta)$ by $\mu_a(\Theta)$ in eq. (4):

$$I_m = K \iint \varphi(r, t)\, dr\, dt \tag{5}$$

where:

$$\varphi(r, t) = \frac{1}{R^2}\, e^{-\mu_o t - \mu_a(\Theta) R}\, f(\cos\Theta)$$

In the present calculations the following values have been used for the absorption coefficient of the primary radiation from Cs^{137} (662 keV) in water $\mu_s = 5.32\ 10^{-2}\ cm^{-1}$, $\mu_a = 3.29\ 10^{-2}\ cm^{-1}$ and $\mu_o = 8.61\ 10^{-2}\ cm^{-1}$. For the electronic cross-section the values ${}_e\sigma_s = 1.59\ 10^{-25}\ cm^2/elec$, ${}_e\sigma_s = 0.98\ 10^{-25}\ cm^2/elec$, ${}_e\sigma = 2.57\ 10^{-25}\ cm^2/elec$ have been chosen. The mean free path of the photons in water using $\eta = 3.35\ 10^{23}\ elec/cm^3$ is 11.6 cm. The Klein-Nishina function has been replaced by:

$$f(\cos\Theta) = (A + C\cos^4\Theta)\ 10^{-27}$$

where:

$A = 5\ cm^2/elec/sterad$ for $0 < \Theta \leq 180°$ or $r \gtrless 0$
$C = 74$ » » $0 \leq \Theta \leq 90°$ or $r > 0$
$C = 0$ » » $0 \leq \Theta \leq 180°$ or $r > 0$

The absorption coefficient $\mu_a(\Theta)$ for the scattered radiation depends upon the angle o scattering and the number of scattering processes. At a scattering angle of 90° the

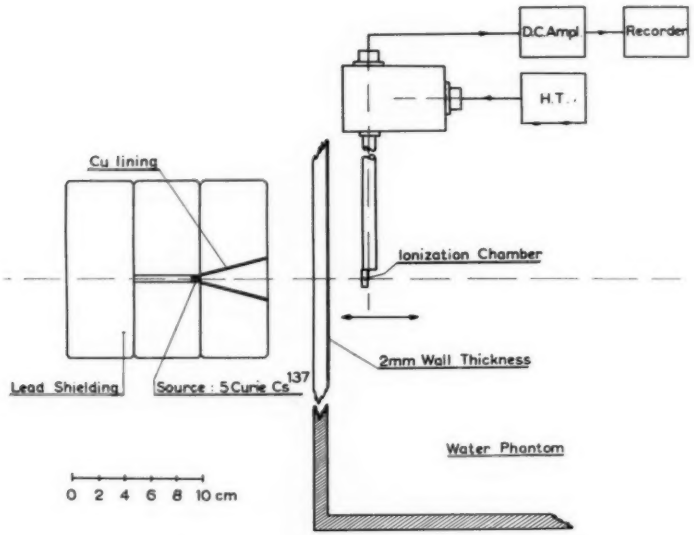

Fig. 1. Experimental arrangement used for measuring depth-dose distributions in water for Cs^{137} (662 keV).

increase in wavelength reduces the energy of the primary radiation to 287 keV and by scattering 180° to 184 keV. Due both to the predominant scattering in the forward direction and the small variation of μ_a within the energy range from 100 keV to 1 MeV, a constant value of $\mu_a(\Theta)$ has been assumed. The value used for this coefficient is $3.29\ 10^{-2}\ cm^{-1}$.

The calculations were carried out for $F = 5$ cm and $F = 10$ cm with $\varphi_o = 30°$ and 18° respectively. The intensity was further calculated for $h = 0, 1, 2, 3, 4, 5, 6, 7$ and 11.6 cm. Eq. (5) was for each value of h integrated over r from $-\infty$ to h.

The numerical integration of eq. (5) was carried out by calculating $\varphi\ (r, t)$ as a function of t for a certain set of r values. Each of these curves was then numerically integrated, and the variation of $\varphi\ (r, t)$ with r was obtained. This procedure was repeated for each value of h.

The radiation intensity along the central axis of the radiation field is composed of radiation from the primary beam and the scattered radiation, which means that even if the primary radiation is mono-energetic, the total intensity at a certain depth will form a spectral distribution which also will change with the depth. At depths less than one mean free path, the main part of the energy absorption in each volume-unit might as a first approximation, be caused by the radiation, which has suffered few collisions. On this assumption the $\mu_a(\Theta)$ has been assumed constant and the conversion of intensity to dose has been done by multiplying the eq. (5) by $\frac{\mu_a}{\varrho}$, where ϱ is the density.

The results are shown in Diagrams 3 and 4.

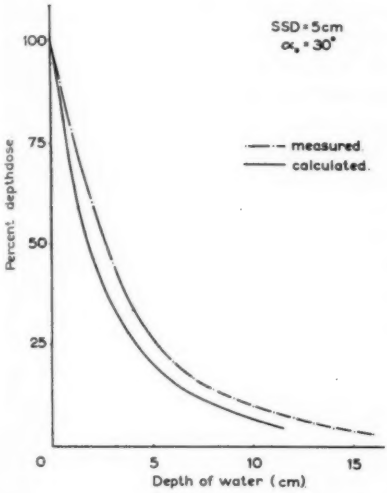

Diagram 7. Experimental and theoretical depth-dose distributions for Cs^{137} for SSD 5 cm.

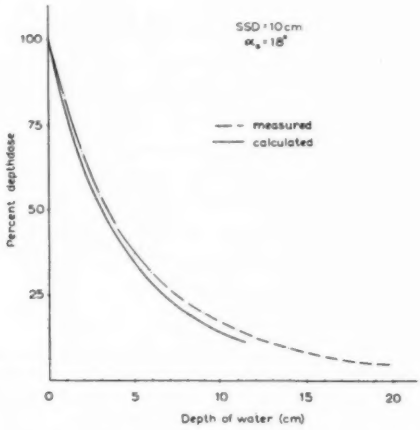

Diagram 8. Experimental and theoretical depth-dose distributions for Cs^{137} for SSD 10 cm.

Measurements of depth-dose distributions

In connection with the theoretical calculations of the depth-dose distribution just described, it was of interest to compare the results with measurements. A 5 curie Cs^{137} source, cylindrically shaped, with a diameter of 3 mm, and 3 mm long, was used for the purpose and its radiation properties were studied using a 1 $^1/_2$" (38 mm) NaJ(Tl) crystal mounted to a 6292 Du Mont photomultiplier. The pulse height distribution was then measured by a RCL 256 channel pulse-analyzer. The detector was exposed using good collimation at a distance of 7 m. The results are shown in Diagram 5, and it is concluded from these measurements that less than 1 % of the activity in the source is due to Cs^{134} emitting higher energies than the 662 keV from Cs^{137}.

The detector used for the dose measurements was made of an air-equivalent plastic scintillator (BELCHER & GEILINGER), with a perspex light guide and a 931A RCA photomultiplier. Studies were carried out on fatigue effect, dose-rate dependence and energy response compared to a Victoreen type ionization chamber. The Cerenkov radiation produced in 2/3 of the light guide by γ-radiation from Cs^{137} (662 keV) was measured to less than 1 % of the crystal response for the same radiation intensity. The dose-rate dependence showed a linear relationship up to

more than 100 r/min. The energy response was studied with a 250 keV roentgen unit using 0.5 mm Cu filter lowering the energy successively. The results are shown in Diagram 6. It is clearly seen from these experiments that the dosemeter should be well suited for dose measurements.

Due to the relatively large size (1 cm) of the scintillation dosemeter the depth-dose measurements in the first 2 cm of the water phantom were carried out using a 0.1 cc ionization chamber. This instrument showed a similar energy response as the scintillation dosemeter (Diagram 6). The first measurements were taken at a depth of 5 mm.

The arrangement used for the depth-dose measurement is shown in Fig. 1. The source was placed in a lead collimator lined with 1.5 mm copper. The entrance surface was given a spherical shape with radius 5 cm at SSD 5 cm, and 10 cm at SSD 10 cm.

The experimental results obtained are shown in Diagrams 7 and 8 for SSD 5 and 10 cm respectively, together with the calculated curves. Comparing the theoretical results with the measured values, the conclusion may be drawn that there is a fair agreement between these curves for SSD 10 cm. At 5 cm there seems to be a rather great deviation. An explanation of this is not easily given since several factors might cause this deviation. In the first place the calculations are approximate. and the experimental arrangement did not completely satisfy the theoretically presumed condition. In this connection the diffusion of radiation through the collimator might have been too large. 5 cm lead will reduce the primary beam to 0.4 ‰. Comparing the agreement between theory and experiment for SSD 10 and 5 cm, the calculation procedure seems to be in better agreement with experiment at a longer SSD.

Acknowledgement

The author wishes to express his sincere thanks to The Norwegian Cancer Society for financial support and to K. Madshus and P. Omsveen for valuable technical assistance.

SUMMARY

Calculations of depth-dose distributions from point sources of Cs^{137} (662 keV) have been carried out for SSD of 5 and 10 cm and opening angles of 60° and 36°, respectively. The dose distribution has been obtained by calculating the dose decrease with depths. caused by the primary radiation, and adding to this the contribution from the scattered radiation. The latter has been evaluated from the integral calculated for the once scattered radiation where an approximation has been introduced in order to include the multiply scattered radiation. The estimated depth-dose distribution has then been compared with experiments using a 5 curie Cs^{137} source.

ZUSAMMENFASSUNG

Berechnungen über die Verteilungen der Tiefendosis von punktförmigen Quellen von ^{137} (662 keV) sind für Quellen-Hautabstände von 5 und 10 cm sowie für Öffnungswinkel n 60° bezw. 36° durchgeführt worden. Die Dosisverteilung wurde durch Berechnung der it zunehmender Gewebetiefe geringer werdenden Strahlendosis, die durch die Primär- rahlung erzeugt wird, und durch Addition des Beitrages der Streustrahlung gewonnen. etztere ist aus dem für einmalig gestreute Strahlung berechneten Integral festgelegt rden; hierbei ist eine Approximation eingeführt worden, um die mehrfach gestreute rahlung einbeziehen zu können. Die so geschätzte Verteilung der Tiefendosis ist dann it Hilfe einer 5 Curie Cs^{137} Quelle experimentell verglichen worden.

RÉSUMÉ

L'auteur a calculé les distributions de doses en profondeur fournies par des sources ponctuelles de Cs^{137} (662 keV) pour les distances source—peau de 5 et 10 cm et pour des angles d'ouverture de 60° et 36°. Il a obtenu la distribution de dose en calculant la dose de rayonnement primaire diminuée du fait de la profondeur, et en y ajoutant la dose due au rayonnement diffusé. Celle-ci a été évaluée au moyen de l'intégrale calculée pour le rayonnement ayant subi une diffusion, en introduisant une approximation pour tenir compte du rayonnement ayant subi plusieurs diffusions. La distribution de dose en profondeur calculée a été comparée aux résultats d'expériences faites avec une source de Cs^{137} de 5 curies.

REFERENCES

Aebersold, P. C.: Importance of isotopes in technology and industry. Peaceful uses of atomic energy 14 (1955), 3.

Baarli, J.: Cesium 137 in plesio- and teletherapy. Atompraxis 4 (1958), 23.

— and Brustad, T.: A 50 curie uranium and tungsten-alloy shielded Cs^{137} plesiotherapy unit. 25. Anniversary book, The Norwegian Radium Hospital (in press).

Belcher, E. H. and Geilinger, J. E.: Improved scintillating media for radiation dosimetry. Brit. J. Radiol. 30 (1957), 103.

Brucer, M.: An automatic controlled pattern cesium 137 teletherapy machine. Amer. J. Roentgenol. 71 (1956), 49.

Cockroft, J.: Atomic energy and its biological applications. Nature 180 (1957), 64.

Lamerton, L. F.: Theoretical study of results of ionization measurements in water with X-ray and γ-ray beams. Brit. J. Radiol. 21 (1948), 276.

Lindell, B. and Walstam, R.: A new telegamma apparatus. Acta radiol. 45 (1956), 236.

Mitchell, J. D.: Practical aspects of radioactive isotopes in relation to medical treatment. Brit. Med. Journ. 2 (1951), 747.

Payne-Scott, R.: Wavelength distribution of scattered radiation in medium traversed by beams of X- or γ-rays. Brit. J. Radiol. 10 (1937), 850.

FROM THE ROENTGEN INSTITUTE (DIRECTOR: PROF. A. ZUPPINGER) UNIVERSITY OF BERN, SWITZERLAND

EFFECT OF 31 MeV GAMMA AND 200 kV ROENTGEN WHOLE-BODY IRRADIATION ON THE NUCLEIC ACID CONTENT OF MOUSE TISSUES

by

Sonja P. Subotič-Nikolić and *Adolf Zuppinger*

The advantages of supervoltage radiotherapy, discussed in an earlier article (20), and its increased application, raise problems concerning the quantitative relations between DMV radiation and conventional roentgen rays. The many articles dealing with this matter have recently been reviewed (4). From these it was evident that no unique relation between the two types of radiation has been found. It is considered, however, (18) that the RBE of a given type of radiation is dependent upon: 1) the test object, 2) the particular response studied and, 3) the time lapse between the irradiation and observation of the effect.

We are naturally primarily interested in an extrapolation of the results of these studies to man; in spite of many technical advantages in carrying out research on simpler systems an investigation on mammals would appear to be the most fruitful.

In view of the marked biological importance (2) and radiosensitivity (6) of nucleic acids, post-irradiation disturbances of the metabolism of these substances appeared to us to merit investigation. The purpose of

Submitted for publication 27 May 1958.

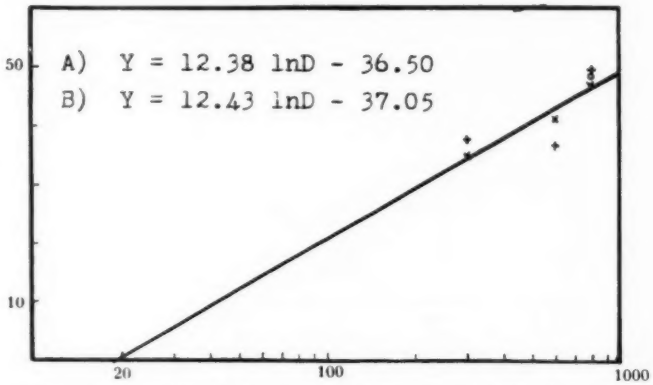

Diagram 1. Percentage diminution of DNA concentration in spleen against the logarithm of the radiation dose. The line corresponds to Picker irradiation. *A* — 200 kV, *B* — 31 MeV.

the present work was therefore twofold: to define simultaneously the behaviour of nucleic acids and their low-molecular derivatives, as reflected in their concentration in three different organs two days after irradiation, and to offer some further contribution to the problem of a comparison of the biological effectiveness of betatron and roentgen rays in mammals.

Experimental

White male mice weighing about 20 g were kept without food for 24 hours before sacrifice in order to counteract any eventual interference of a diminished food intake by the irradiated animals; water was allowed ad libitum. The mice were sacrificed by decapitation under light ether anesthesia. The organs were dissected, washed twice in cold physiologic saline, and dried on filter paper; two livers, 4—5 spleens, and 4—5 thymus were, as a rule, pooled. The organs were immediately weighed and then frozen. Homogenization and extraction of acid-soluble substances proceeded in a cold room at about 0° C. Perchloric acid (14) was employed as an extraction medium. An acid-soluble fraction was obtained after a 20 min extraction of homogenized tissue in 1 % perchloric acid and centrifugation in a high speed refrigerator centrifuge; the remainder was extracted for an hour at boiling point in 5 % perchloric acid.

A Beckmann apparatus (model B and DU) was used for the spectrophotometric analyses; optical densities of acid-soluble fractions were measured at 260 mμ.

Quantitative analyses of DNA and RNA were made by the CERIOTTI (3) and MEJBAUM (13) methods, respectively.

The experiment was performed in a total of about 550 mice, 175 of which were not irradiated and which served as controls.

The animals were irradiated with ionizing radiations of two energies. The 200 kV radiation of a Picker unit was fractioned at 50 impulses per sec exactly as the 31 MeV

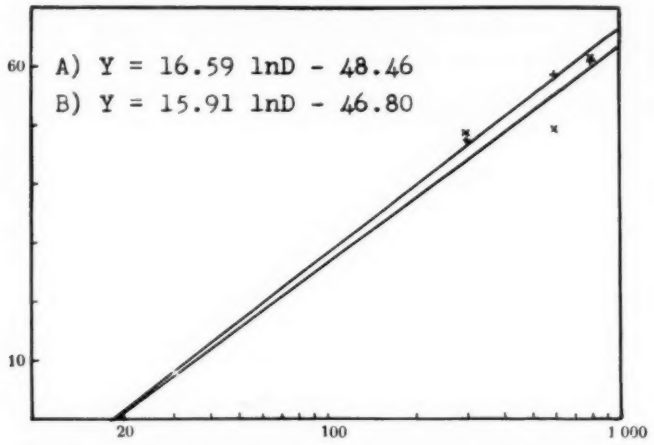

Diagram 2. Percentage diminution of DNA concentration in thymus against the logarithm of the radiation dose. *A* — 200 kV, *B* — 31 MeV.

radiation of our Brown-Boveri betatron. A group of mice was irradiated at 200 kV with an apparatus of the Greinacher type, which delivers non-fractioned rays; the radiation dose corresponding to the middle of the body of a mouse was determined by a Victoreen chamber.

The depth dose curve for betatron gamma rays, measured in water or in a plexiglass phantom, showed an ionization maximum between 4.5 and 6.5 cm (± 1 %). As the animals (about 2 cm thick) were irradiated at a depth of 4 cm behind plexiglass, the dose through the whole body was obviously constant at 1 %.

In order to compensate for inhomogeneities in the betatron and roentgen unit fields all animals were irradiated on a rotating plate. The dose rate, about 15r/min, was the same for all three types of radiation and the animals were irradiated at three dose levels: 300r, 600r and 800r. The animals were sacrificed after 48 hours.

Results

The results are expressed as the contents of nucleic acids per gram of fresh tissue in terms of a percentage of corresponding control values; they are also presented as a percentage diminution of nucleic acid concentration. Extinctions of acid-soluble fractions at 260 mμ (corresponding to 10 mg tiss./ml) are expressed as a percentage of the corresponding control values.

Experimental points corresponding to 200 kV non-fractioned and ultra-fractioned roentgen rays and to 31 MeV gamma radiation are represented by the symbols 0, +, and x, respectively. Standard deviations of the observations have been mostly of the order of 10 to 15 %.

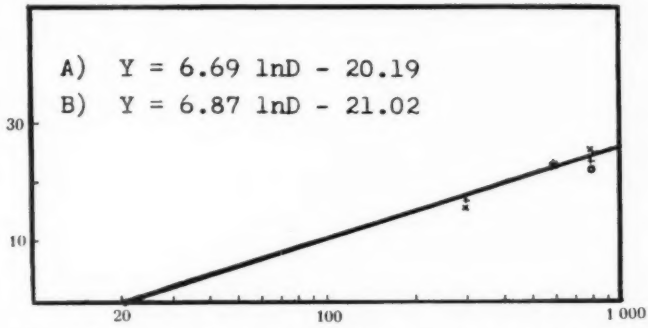

Diagram 3. Percentage diminution of RNA concentration in spleen against the logarithm of the radiation dose. The line corresponds to Picker irradiation. *A* — 200 kV, *B* — 31 MeV.

The most satisfactory siting of the experimental points has been calculated by supposing that the effect studied has been a linear function of the logarithm of the radiation dose (8); a threshold dose of about 20r has been predicted.

Equations of regression lines corresponding to the effects of 200 kV ultrafractioned roentgen rays and 31 MeV gamma rays are represented by (A) and (B), respectively (Diagrams 1, 2, and 3).

It was first determined whether ultra-fractioning (10) at the single energy level influenced the biologic effect observed. As shown by our results (Diagrams 1 to 3 and the Table below) practically no differences between data obtained by the constant and alternative potential unit operated at 200 kV were found. It may also be seen that no appreciable differences were found in comparing effects of the latter and betatron gamma-rays shown by equations of regression lines. In case of spleen DNA and RNA, regression curves almost coincide, and in case of thymus DNA the small difference between the two curves is also of no statistical significance.

A drastic reduction of nucleic acid concentration after irradiation in

Table

Effect of 800r of 200 kV roentgen rays on nucleic acid content in liver

	Control	Picker irradiation	Greinacher irradiation
DNA	100 ± 6.5	94.1 ± 11.1	91.5 ± 7.8
RNA	100 ± 12.6	106.7 ± 10.9	108.6 ± 11.4
Extinction of acid-soluble fraction	100 ± 7.4	102.4 ± 9.9	99.4 ± 9.6

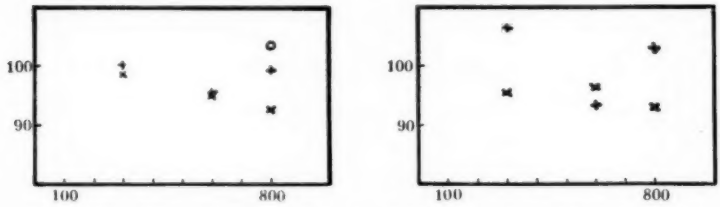

Diagram 4. a) Percentage extinctions of acid-soluble fractions of the spleen against the radiation dose. b) Similar plotting corresponding to thymus.

two of the organs studied is to be explained by a decrease in a new formation of DNA (11) (*e. g.* by inhibition of the doubling of the DNA content per nucleus which precedes the cell division) on the one hand, and by the destruction of DNA by increased activity of deoxyribonuclease (15) on the other. In this connection the investigation of MAIN, COLE and ELLIS (12), in which they showed that soluble deoxypolynucleotides are released in the spleen 6 hours after irradiation, should be mentioned.

From the results presented markedly different post-irradiation responses of the DNA in the liver to those in the spleen and thymus are evident. While an irradiation with 800r resulted in a diminution of the DNA content of about 50 % and 60 % in the spleen and thymus, respectively, only a slight change, if any, was found in the liver. Similar phenomena has also been noted in the case of RNA, where under equal conditions of irradiation certainly no depletion of RNA has been revealed in the liver, while the spleen showed a distinct diminution in the content of the substance. The responses of the three organs studied are not surprising in view of their different DNA renewal rate (5), (17), the post-irradiation disturbance of which is more marked in organs with higher cell division rates.

Diagram 4 shows no appreciable quantitative post-irradiation alterations of acid-soluble purine and pyrimidine derivatives, which are probably related to nucleic acid precursors. (As a result of regression, the lines with coefficients of a slope not significantly differing from zero were obtained.) This suggests that inhibition of nucleic acid synthesis does not take place at its initial level, but rather at a macromolecular one (19). Other studies (1), (16) with radioactive methods may be cited in favour of the conception that irradiation does not affect the metabolism of the acid-soluble constituents in question.

An explanation of the mechanism of the inhibition of DNA polymerization would be that nucleotide phosphorylations (which, according to LIPMANN (7) are indispensable for their combination in DNA) are disturbed (9).

Acknowledgements

The authors wish to thank Dr. W. Minder, Dr. G. Poretti, and Dr. E. Linder, for their valuable advice, the Theodor Kocher Institute for technical facilities, and the Swiss Atomic Energy Commission and the Brown-Bovery Betatron Company for their support of this investigation.

SUMMARY

A comparative study of the effects of 31 MeV gamma and 200 kV roentgen rays on nucleic acids and their low-molecular derivatives content in mouse spleen, thymus and liver was performed. No significant differences could be proved in the radiation response of these substances, suggesting that the ratio of intensity of the biologic effect studied was near unity for the two energies in question.

ZUSAMMENFASSUNG

Eine vergleichende Studie der Wirkung von 31 MeV-Gammastrahlen und von 200 kV-Röntgenstrahlen auf Nukleinsäuren und deren kleinmolekuläre Derivate, welche in der Milz, der Thymus und der Leber der Maus enthalten sind, ist durchgeführt worden. Es konnten keine signifikativen Unterschiede in der Strahlenreaktion auf diese Substanzen nachgewiesen werden. Es ergab sich demnach, dass das Verhältnis der Intensität des untersuchten biologischen Effektes für die beiden in Frage stehenden Energien nahezu gleich war.

RÉSUMÉ

Les auteurs ont fait une étude comparative de l'effet des rayons gamma de 31 MeV et des rayons roentgen de 200 kV sur la teneur de la rate, du thymus et du foie de la souris en acides nucléiques et en leurs dérivés de bas poids moléculaire. Ils n'ont pas pu prouver de différence significative dans l'effet de ces radiations sur ces substances, ce qui fait penser que le rapport des intensités de l'effet biologique étudié est voisin de l'unité pour les deux énergies en question.

REFERENCES

1. Benet, E., Kelly, L. and Krueckel, B.: Effect of X-irradiation upon the incorporation of adenine -4, 6-C^{14} in mice. Fed. Proc. 13 (1954), 181.
2. Brachet, J.: Le rôle des acides nucléiques dans la vie de la cellule et de l'embryon. Actual. biochim. No. 16. Edit. Desoer, Liège 1952.
3. Ceriotti, G.: A microchemical determination of desoxyribonucleic acid. J. Biol. Chem. 198 (1952), 297.
4. Gunter, Sh., Kohn, H., Tyree, E., Laughlin, J., Ovadia, J., Shapiro, G. and Thompson, P.: The relative biological effectiveness of 180-KeVp and 22.5-MeVp X-rays determined from the dose-survival curve of saccharomyces cerevisiae. Rad. Res. 4 (1956), 326.

5. HAMMARSTEN, E. and HEVESY, G.: Rate of renewal of ribo- and desoxyribonucleic acids. Acta physiol. scand. 11 (1946), 335.
6. HEVESY, G.: On the effect of roentgen rays on cellular division. Rev. mod. Phys. 17 (1945), 102.
7. JONES, M., LIPMANN, F., HILZ, H. and LYNEN, F.: On the enzymatic mechanism of coenzyme A acetylation with adenosine triphosphate and acetat. J. Am. Chem. Soc. 75 (1953), 3285.
8. KALLMAN, R. and KOHN, H.: The reaction of the mouse spleen to X-rays measured by changes in organ weight. Rad. Res. 3 (1955), 77.
9. KANAZIR, D. et ERRERA, M.: Métabolisme anaérobique de l'adénosine triphosphate (ATP) et de l'acide désoxyribonucléique (ADN) chez E. Coli après irradiation U. V. Biochim. biophys. Acta 16 (1955), 477.
10. KEPP, K.: Zusammenhänge zwischen Ionisationsdichte and Zeitfaktorwirkung. Strahlentherapie 92 (1953), 590.
11. LAVIK, P. and HARRINGTON, H.: Some biochemical effects of radiation on lymphatic tissue. NYO (Rochester, New York University) 1951, p. 1626.
12. MAIN, R., COLE, L. and ELLIS, M.: Chromatographic characterization of soluble deoxypolynucleotides released in mouse spleen by X-irradiation. Nature 180 (1957), 1285.
13. MEJBAUM, W.: Über die Bestimmung kleiner Pentosemengen, insbesondere in Derivaten der Adenylsäure. Z. physiol. Chemie 258 (1939), 117.
14. OGUR, M. and ROSEN, G.: The nucleic acids of plant tissues. I. The extraction and estimation of desoxypentose nucleic acid and pentose nucleic acid. Arch. Biochem. 25 (1950), 262.
15. OKADA, S., GORDON, E., KING, R. and HEMPELMANN, L.: The effect of X-rays exposure on deoxyribonuclease II activity in lymphatic tissues. Arch. Biochem. 70 (1957), 469.
16. SHERMAN, F. and FORSSBERG, A.: Incorporation of P^{32} into TCA fractions of liver from irradiated and non-irradiated mice. Arch. Biochem. 48 (1954), 293.
17. STEVENS, C., DAOUST, R. and LEBLOND, C.: The desoxyribonucleic acid of interphase and dividing nuclei. Canad. J. Med. Sci. 31 (1953), 263.
18. STORER, J., HARRIS, P., FURCHNER, J., et coll.: The relative biological effectiveness of various ionizing radiations in mammalian systems. Rad. Res. 6 (1957), 188.
19. SUBOTIĆ, S., KAČANSKI-BELOS, K. and KANAZIR, D.: Effects of U. V. irradiation on metabolism of nucleic acids in salmonella typhimurium. Bull. Inst. Nuclear Sci. 6 (1956), 193.
20. ZUPPINGER, A., COTTIER, H., GLAUSER, O., et coll.: Die ultraharten Strahlungen zur Krebsbehandlung. Rad. Clin. 24 (1955), 65.